Ma *et al. Soft Sci* 2024;4:26
DOI: 10.20517/ss.2024.20

Soft Science

Review Article

Open Access

Check for updates

Recent advances in laser-induced-graphene-based soft skin electronics for intelligent healthcare

Zhiqiang Ma[1,2,*], **Bee Luan Khoo**[1,2,3,*]

[1]Department of Biomedical Engineering, City University of Hong Kong, Hong Kong 999077, China.
[2]Hong Kong Center for Cerebro-Cardiovascular Health Engineering, Hong Kong 999077, China.
[3]City University of Hong Kong Futian - Shenzhen Research Institute, Shenzhen 518057, Guangdong, China.

[*]**Correspondence to:** Dr. Zhiqiang Ma, Prof. Bee Luan Khoo, Department of Biomedical Engineering, City University of Hong Kong, 83 Tat Chee Avenue, Kowloon Tong, Hong Kong 999077, China. E-mail: zqma@hkcoche.org; blkhoo@cityu.edu.hk

How to cite this article: Ma Z, Khoo BL. Recent advances in laser-induced-graphene-based soft skin electronics for intelligent healthcare. *Soft Sci* 2024;4:26. https://dx.doi.org/10.20517/ss.2024.20

Received: 7 May 2024 **First Decision:** 4 Jun 2024 **Revised:** 25 Jun 2024 **Accepted:** 28 Jun 2024 **Published:** 9 Jul 2024

Academic Editor: YongAn Huang **Copy Editor:** Pei-Yun Wang **Production Editor:** Pei-Yun Wang

Abstract

Skin is a rich source of invaluable information for healthcare management and disease diagnostics. The integration of soft skin electronics enables precise and timely capture of these cues at the skin interface. Leveraging attributes such as lightweight design, compact size, high integration, biocompatibility, and enhanced comfort, these technologies hold significant promise for advancing various applications. However, the fabrication process for most existing soft skin electronics typically requires expensive platforms and clean-room environments, potentially inflating production costs. In recent years, the emergence of laser-induced-graphene (LIG) has presented a practical solution for developing soft skin electronics that are both cost-effective and high-performing. This advancement paves the way for the widespread adoption of intelligent healthcare technologies. Here, we comprehensively review recent studies focusing on LIG-based soft skin electronics (LIGS^{2}E) for intelligent healthcare applications. We first outline the preparation methodologies, fundamental properties of LIG, and standard regulation strategies employed in developing soft skin electronics. Subsequently, we present an overview of various LIGS^{2}E designs and their diverse applications in intelligent healthcare. These applications encompass biophysical and biochemical sensors, bio-actuators, and power supply systems. Finally, we deliberate on the potential challenges associated with the practical implementation of LIGS^{2}E in healthcare settings and offer insights into future directions for research and development. By elucidating the capabilities and limitations of LIGS^{2}E, this review aims to contribute to advancing intelligent healthcare technologies.

Keywords: Skin electronics, laser-induced-graphene, soft sensors, intelligent healthcare

INTRODUCTION

As the human's largest organ, the skin provides abundant physiological information for health management[1,2]. For instance, skin mechanical deformations reflect health status, including cardiovascular health[3,4], expressions[5,6], and joint movements[7,8], and sweat at the skin interface contains a series of biochemical biomarkers, including lactate[9], cortisol[10], *etc.* Accurate and real-time monitoring of these indicators provides users and doctors with important information for precise healthcare[11-13]. Most existing clinical devices for detecting these indicators exhibit shortcomings, such as high cost, large volume, low comfort, discontinuous monitoring, *etc.* Various soft skin electronics have been developed to address these challenges, characterized by cost-effectiveness, small size, high comfort, and continuous detection capabilities. These devices have been fabricated using diverse techniques[14,15], including traditional lithography[16] and printing technology[17,18]. However, complicated processing, expensive platforms, and clean-room environments are required to fabricate most of these soft skin electronics, which increase the economic cost and hinder the widespread applications of intelligent healthcare.

The laser engraving strategy showcases overpowering manufacturing advantages in effective cost due to one-step processing and clean-room-free, as well as performance superiority in uniformity and repeatability originating from precise programmable features. There are various soft skin electronics fabricated by laser techniques, including laser sintering of metal nanomaterials[19], laser processing of conductive polymers[20], and laser producing of functional materials[21]. Polyimides (PI) are widely utilized in flexible electronics, profiting from their remarkable physicochemical properties, such as high mechanical strength and thermal and chemical stability[22]. Laser engraving with a PI sheet can produce porous graphene, termed laser-induced-graphene (LIG)[23]. Laser processing parameters, including laser powers, speeds, and pulse density, can regulate the morphology of LIG. The fabricated LIG exhibits excellent conductivity (square resistance < 10 Ω)[24,25] and a large superficial area of 340 m^2/g[23]. The overall pattern of LIG can be precisely programmed using computer design. In addition, this processing method is green because it can be finished in ambient conditions with negligible waste generated. All these advantages inspire researchers to fabricate various LIG-based flexible devices for broad applications, including soft sensors[26-28], RF (radio frequency) circuits[29], functional surfaces[30], energy storage[31], soft robotics[32], *etc.*

This review mainly discussed the recent advances in LIG-based soft skin electronics (LIGS²E) for human health management, emphasizing engineering design strategies and intelligent applications. Based on the preferred reporting items for systematic reviews and meta-analyses (PRISMA) process[33], this study mainly summarized and reviewed the literature from January 2014 to January 2024. Following a rigorous screening process, a total of 86 articles were thoroughly assessed and subsequently included in this comprehensive review. As illustrated in Figure 1[3,26,34-50], the preparation strategies and the regulatory approaches of LIG for soft skin electronics are reviewed first. Following this, various applications of LIGS²E for intelligent healthcare are reviewed, including biosensors (biophysical and biochemical sensors) and bio-actuators, power supply, multimodal sensing realization, and artificial intelligence integration. Finally, the potential challenges and futural outlook of LIGS²E for intelligent healthcare are discussed.

SYNTHESIS AND REGULATION STRATEGIES OF LIG

Fabrication and properties of LIG

In 2014, Lin *et al.* discovered accidentally that a commercial CO_2 infrared (IR) laser (wavelength: 10.6 μm) could transform PI film into porous graphene in ambient conditions[23]. As shown in Figure 2A, the localized high temperatures induced by the instant laser irradiation can rearrange carbon atoms to porous LIG structures by breaking C–O, C=O, and N–C bonds. The patterns of LIG can be precisely regulated by the programmable computer design without using a mask. Benefiting from the thermal effect, the LIG

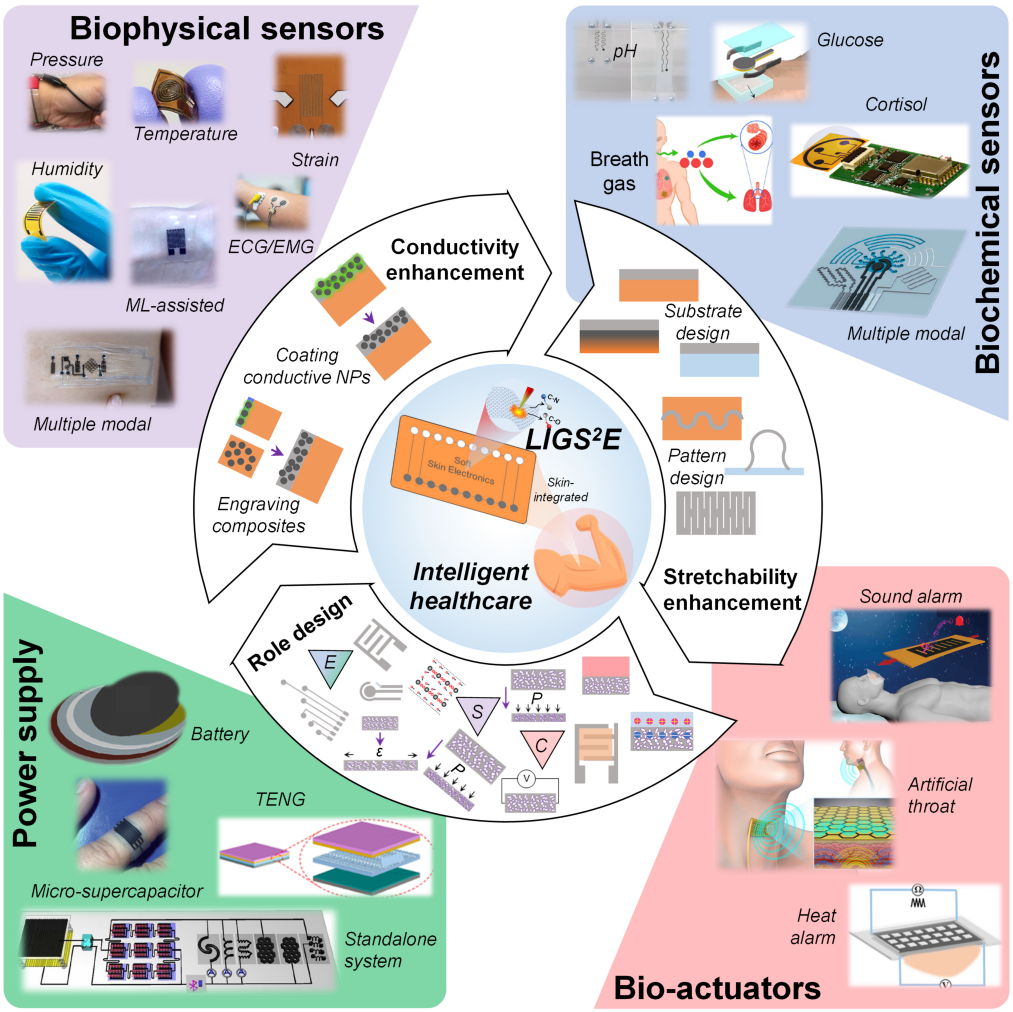

Figure 1. Schematic illustrating LIGS^{2}E for intelligent healthcare. Porous LIG is employed in three leading roles (S, sensing element; E, electrode; C, conductor) to develop various flexible skin-integrated electronics (biophysical sensors, biochemical sensors, bio-actuators, and power supply) for intelligent healthcare. Copyright 2023, Cell Press[3]. Copyright 2023, Springer Nature[26]. Copyright 2020, American Chemical Society[34]. Copyright 2020, WILEY-VCH[35]. Copyright 2018, WILEY-VCH[36]. Copyright 2018, WILEY-VCH[37]. Copyright 2020, Elsevier B.V[38]. Copyright 2022, Springer Nature[39]. Copyright 2021, Elsevier B.V[40]. Copyright 2017, American Chemical Society[40,41]. Copyright 2022, Springer Nature[41,42]. Copyright 2020, Cell Press[43]. Copyright 2019, Wiley-VCH GmbH[44]. Copyright 2020, American Chemical Society[45]. Copyright 2023, Springer Nature[46]. Copyright 2022, AIP Publishing[47]. Copyright 2019, Elsevier B.V.[48]. Copyright 2019, Springer[49]. Copyright 2017, Wiley-VCH GmbH[50]. LIGS^{2}E: LIG-based soft skin electronics; LIG: laser-induced-graphene.

exhibits porous structures [Figure 2B], which probably enhances the sensing performance of LIG-based soft sensors. Different from pure PI films, the Raman spectra of LIG showcase three prominent peaks at 1,312 cm^{-1} (D-band), 1,598 cm^{-1} (G-band), and 2,612 cm^{-1} (2D-band) [Figure 2B]. The 2D peak occurs due to defects and damaged sp_2 C–C bonds, and the G peak is related to graphite-derived structures. The sharp 2D peak dominates in monolayer graphene, which is probably raised from graphene structures resulting from laser processing. The introduction of graphene flakes endows LIG-based devices with specific electronic conductivity. Besides IR laser, other laser sources, including visible and ultraviolet (UV), facilitate LIG. It is worth mentioning that the LIG developed by the UV laser exhibits better uniformity and higher resolution than that prepared by the IR laser. In addition to traditional PI sheets, other aromatic polymers, including polyetherimide (PEI)[51], poly(ether sulfone) (PES)[52], poly (ether ether ketone) (PEEK)[53], and

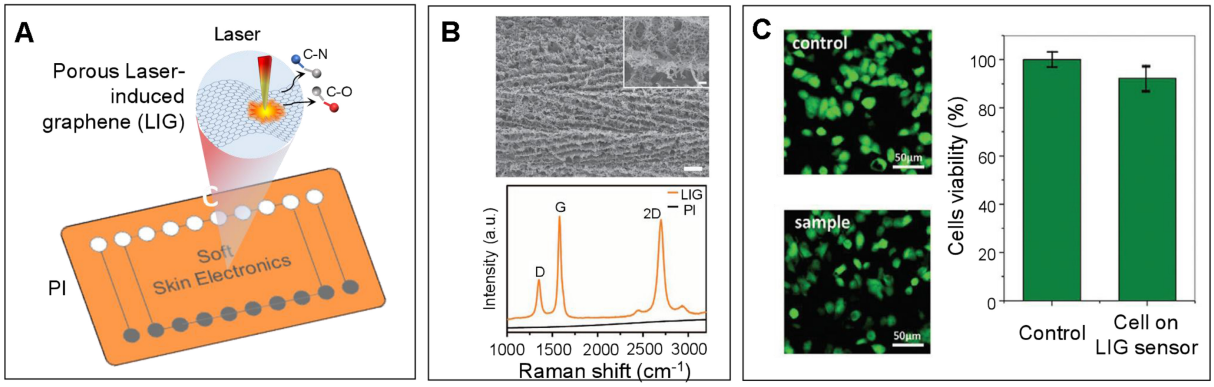

Figure 2. Preparation and regulation strategies of LIG for soft skin electronics. (A) Schematic illustrating the preparation of LIG; (B) Micromorphology and chemical elements analysis of LIG. Reproduced with permission[23]. Copyright 2014, Springer Nature; (C) Biocompatibility results of LIG. Reproduced with permission[60]. Copyright 2020, WILEY-VCH. LIG: Laser-induced-graphene.

green environment-friendly materials, including wood[25], leaf[54], paper[55], and food[56], are successfully utilized to prepare LIG. Besides the traditional 2D pattern, the LIG can be fabricated in a 3D fiber configuration using a laser pyrolytic jetting process[57].

Due to close interaction with human skin, soft skin electronics are required to exhibit excellent biosafety and biocompatibility, avoiding allergies and other discomfort. Previous studies revealed that skin irritation was almost negligible after a long-term integration of LIG-based devices onto the skin surface[58,59]. Meanwhile, Kaidarova *et al.* evaluated the biocompatibility of LIG through cytotoxicity assays and fluorescent staining[60]. The fluorescent photographs showcased that the HCT 116 cells could grow on the LIG sensor in a confluent manner [Figure 2C]. As expected, the cell viability maintained was higher than 90%, exhibiting no negligible difference from the control group after 24 h of incubation. In addition, d'Amora *et al.* conducted a comprehensive assessment of the biosafety of LIG by administering various concentrations of LIG into zebrafish embryos and evaluating its effects on key biological parameters, including embryo viability and morphological changes[61]. The findings demonstrated that LIG had no discernible impact on zebrafish development or the activities, such as swimming and cardiac function, of the treated zebrafish. These results provide direct evidence of the biocompatibility of LIG. Besides its remarkable biocompatibility, LIG showcased remarkable antibacterial and antiviral properties. Huang *et al.* investigated the bacterial killing efficiency of LIG using *Escherichia coli* (*E. coli*) as a model, achieving an efficiency of approximately 81%. Furthermore, when combined with the photothermal effect, the bacterial killing efficiency was further improved to 99.998%[62]. Additionally, when examining human coronaviruses (HCoV-OC43 and HCoV-229E) as models, LIG exhibited a high inhibition rate of over 95% against these coronaviruses[63]. The obtained results collectively confirmed the remarkable biocompatibility of LIG materials, thereby ensuring their biosafety in various bioengineering applications.

Regulation strategies of LIG for soft skin electronics

For soft skin electronics development, LIG must be regulated with suitable properties or patterns. This section mainly discusses the enhancement strategies of electric conductivity and stretchability and the roles design of LIG in soft skin electronics.

Conductivity enhancement

The conductivity of LIG can be regulated by engraving parameters and blended strategies [Figure 3A]. Benefiting from the laser engraving strategy, the conductivity of LIG is precisely controlled by laser

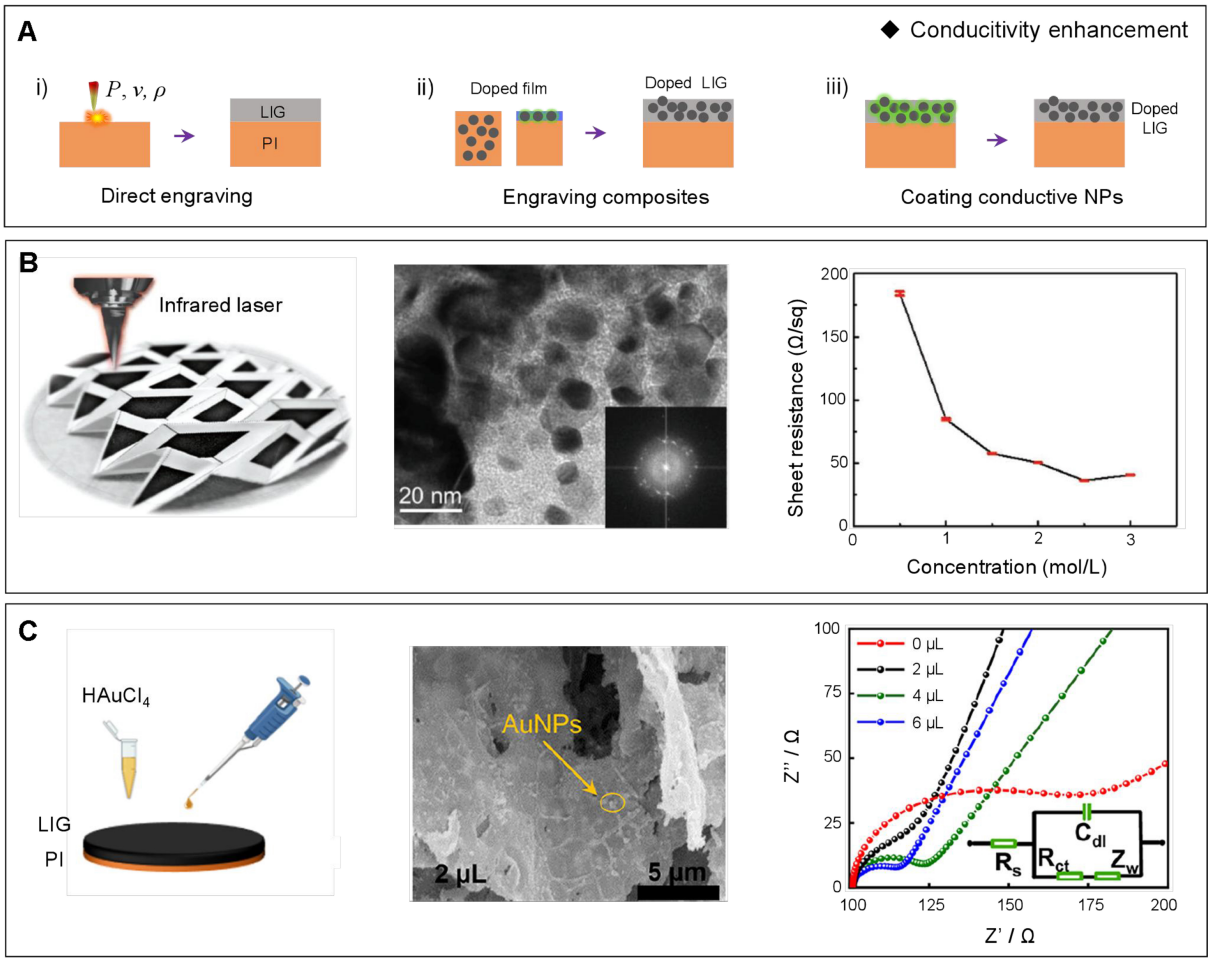

Figure 3. Conductivity enhancement strategies of LIG. (A) Schematic illustration exhibits the conductivity regulation strategies of LIG; (B) A mechanically stable Mo_3C_2@LIG electrode developed by laser engraving a modified composite[69]. Copyright 2018, WILEY-VCH; (C) An AuNPs@LIG electrode is prepared by coating and heating treatments[71]. Copyright 2022, American Chemical Society. LIG: Laser-induced-graphene.

processing parameters, including laser wavelength, pulse duration, laser power, scanning speed, *etc.*[51]. A portion of laser energy is absorbed by substrates irradiated by a laser beam, converting into local high thermal energy and heating the substrates. Thus, the laser wavelength can affect the light absorption efficiency of substrates and, thereby, the production efficiency of LIG. The laser wavelength for LIG preparation [including < 400 nm (UV), 400-750 nm (visible), 0.74-2.5 μm (near-infrared), 2.5-25 μm (mid-infrared)] can be optimized by determining the most efficient wavelength range strongly absorbed by substrates[64].

Meanwhile, the laser duration can affect the formation of LIG. It revealed that the LIG could be prepared by various lasers with different pulse durations, such as continuous waves[65], millisecond lasers[66], microsecond lasers[23], nanosecond lasers[35], *etc.* Short pulse duration generates thin heat-affected zones, benefiting the high spatial resolution LIG fabrication. After the determination of laser type, the conductivity of LIG can be precisely controlled by laser power and scanning speed. For instance, the sheet resistance of the LIG, prepared by CO_2 laser engraving PI substrate, was within a range of 5-115 Ω/sq[67]. The sheet resistance of LIG decreased with increased laser power. However, the excessive laser power decreased conductivity, originating from an increase in the graphitic tracks' defect level or the graphene's oxidation[68]. High

scanning speed could compensate for this defect while benefiting large-scale production[54].

To enhance the conductivity further, researchers have proposed a blended strategy. It can be divided into two types: laser engraving substrates blended with conductive sources and LIG with conductive sources. Before laser engraving treatment, doping the substrate with conductive nanoparticle sources is an effective approach to improve the electrical properties of LIG. For instance, Zang *et al.* developed a mechanically stable Mo_3C_2@LIG electrode by laser engraving a fibrous paper soaked with gelatin-mediated inks rich in molybdenum ions[69] [Figure 3B]. The prepared Mo_3C_2@LIG electrodes showcased high conductivity (~30 Ω/sq) and fascinating porous structures, exhibiting potential applications, including biochemical sensors, energy harvesters and supercapacitors.

Meanwhile, modification of fabricated porous LIG with conductive nanoparticles (such as Ag paste[39], silver nanowires (AgNWs)[70], Au[40,47,71], Ni[40], polyaniline (PANI)[41], carbon nanotubes (CNT)[72], MXene[73], and MXene-Ti_3C_2Tx@3, 4-ethylene dioxythiophene (EDOT)[74]) or conductive polymers [for example, poly(3,4-ethylenedioxythiophene) (PEDOT)[75]] can significantly improve the conductivity of electrodes. For instance, Huang *et al.* reported a gold nanoparticles (AuNPs)@LIG electrode prepared by coating a chloroauric acid ($HAuCl_4$) onto the porous LIG electrode and then baked in the thermostatic oven[71] [Figure 3C]. The fabricated AuNPs@LIG electrodes showcased a low impedance of 16 Ω, facilitating the electron transfer between the enzyme active center and electrode surface, endowing the device's better performance. Meanwhile, Yang *et al.* developed a stretchable AgNWs electrode by spray-coating an AgNWs solution on a prestressed LIG/polydimethylsiloxane (PDMS)-Ecoflex substrate and then releasing the substrate[70]. Profited from the evenly distribution AgNWs on the 3D porous LIG/PDMS-Ecoflex substrate and a pre-strain (30%) design, the conductivity of the LIG electrodes reduced from 48.6 to 3.2 Ω/sq.

Stretchability enhancement

Human skin exhibits natural strain up to 50%-80%[76]. Therefore, stretchability is important in soft skin electronics to withstand daily skin deformations while maintaining stable performance. Several engineering strategies are utilized to realize high stretchability [Figure 4A]. Due to the thermoplastic property of the PI film, the LIG directly fabricated on PI sheets showcased limited stretchability (up to 10%)[42,44,77]. This limited stretchability hinders the development of high-fidelity soft skin electronics. To tackle this problem, researchers have attempted several mechanical strategies to improve the stretchability of LIG/PI composites, including kirigami[78], serpentine patterns[41], and 3D architectures[79]. For example, Ling *et al.* reported a straightforward and practical strategy for developing LIG's 3D hierarchical architectures with designed configurations through mechanically guided and 3D assembly[79]. The resulting device with 3D helical coils exhibited negligible variations in electrical resistance when stretched to 150%. The electrical resistance only increased by approximately 0.3%, even after undergoing 1,000 biaxial stretching cycles with a strain of 50%.

To further improve the stretchability of LIG functional composites, the elastomers containing carbon sources were employed to be thermal treatment with laser to prepare LIG, such as PDMS[80] directly, PDMS/PI composites[81], PDMS/photosensitive PI (PSPI) composites[82], *etc.* For instance, Wang *et al.* utilized PDMS/PI composites, prepared by blending PI particles in PDMS precursors, to develop LIG-based stretchable and soft electronics[81]. Benefiting from the flexible and stretchable properties of the PDMS/PI composites, the fabricated LIG-based flexible electronics exhibited outstanding mechanical stretchability (> 15%).

Finally, transferring prepared LIG from the PI substrate to a stretchable elastomer substrate provides a practical approach to developing soft skin electronics. The stretchability of resulting LIG/elastomer

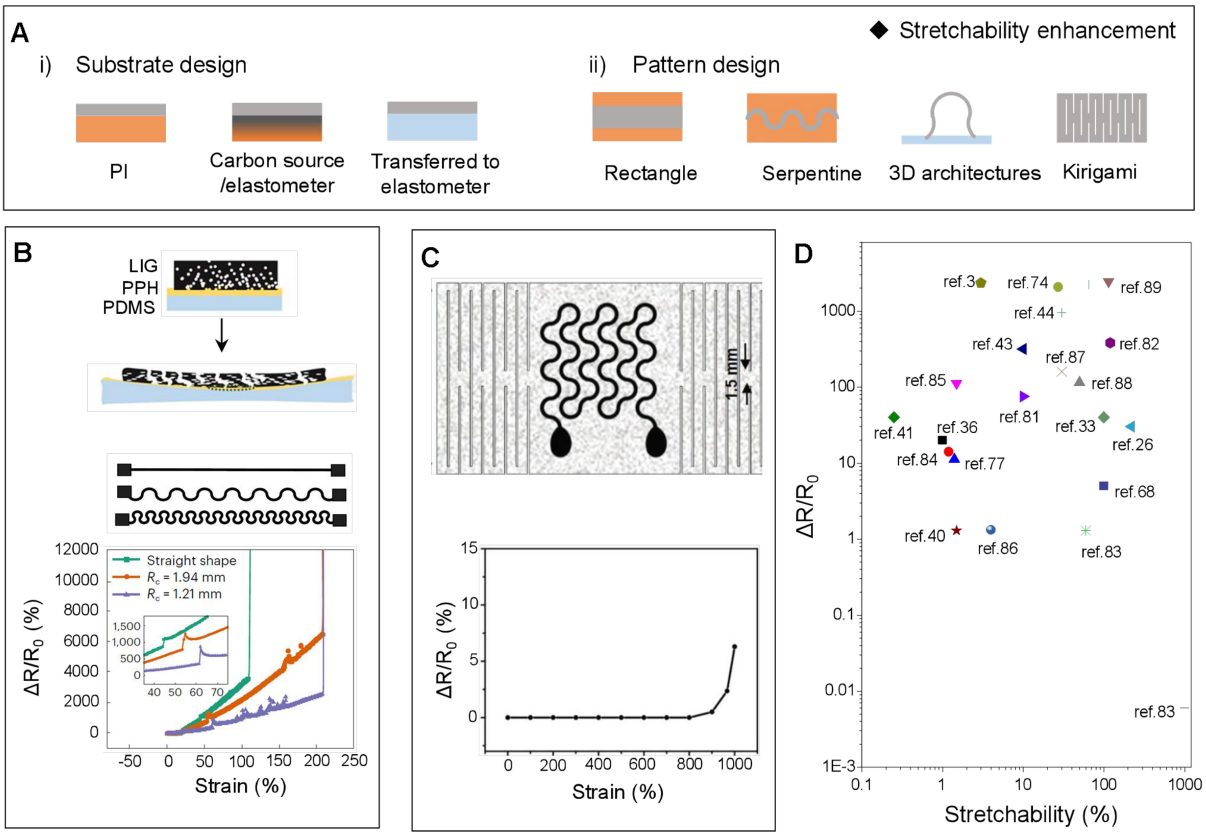

Figure 4. Stretchability enhancement strategies of LIG. (A) Schematic illustration exhibits LIG's stretchability regulation strategies; (B) Serpentine LIG is transferred onto a soft, stretchable hydrogel layer[27]. Copyright 2023, Springer Nature; (C) A kirigami-patterned PDMS sponge with transferred porous LIG[83]. Copyright 2020, WILEY-VCH; (D) Electromechanical response comparison of typical LIG composites. LIG: Laser-induced-graphene; PDMS: polydimethylsiloxane.

composites depends on the material properties of the elastomer. For example, a commercial medical polyurethane film (MPU) is widely used for wound healthcare, exhibiting several advantages, including high stretchability (> 100%), long-term and conformal attachment on the skin (> 72 h), gas permeability, *etc.* These features enable it to be a potential substrate for skin electronics development. Motivated by this, Dallinger *et al.* transferred porous LIG from a PI substrate onto an ultrathin MPU film (~50 μm in thickness), achieving a remarkable stretchability (> 100%) and long-term stability in electromechanical tensile tests (> 200 cycles)[34]. Furthermore, introducing mechanical design in elastomer enhances the stretchability of LIG/elastomer composites, such as serpentine design[27] and kirigami configuration[83]. For instance, Lu *et al.* transferred prepared serpentine LIG onto a soft and stretchable hydrogel layer, achieving a high stretchability up to approximately 220% [Figure 4B][27]. In addition, Sun *et al.* transferred porous LIG onto a PDMS sponge with a kirigami pattern to improve the stretchability, originating from the fact that the kirigami cuts could tolerate the applied strains[83]. As expected, the electrical resistance of the LIG/PDMS sponge only increased by approximately 6%, even when stimulated by a tensile strain of 1,000% [Figure 4C]. Figure 4D illustrates the strain range and electromechanical sensitivity of typical LIG composites[3,26,33,36,40,41,43,44,68,74,77,81-89].

Role design of LIG in soft skin electronics

For the development of soft skin electronics, versatile LIG plays three leading roles, including sensing materials, electrodes, and conductors [Figure 5]. The densely interconnected graphene flakes endow porous

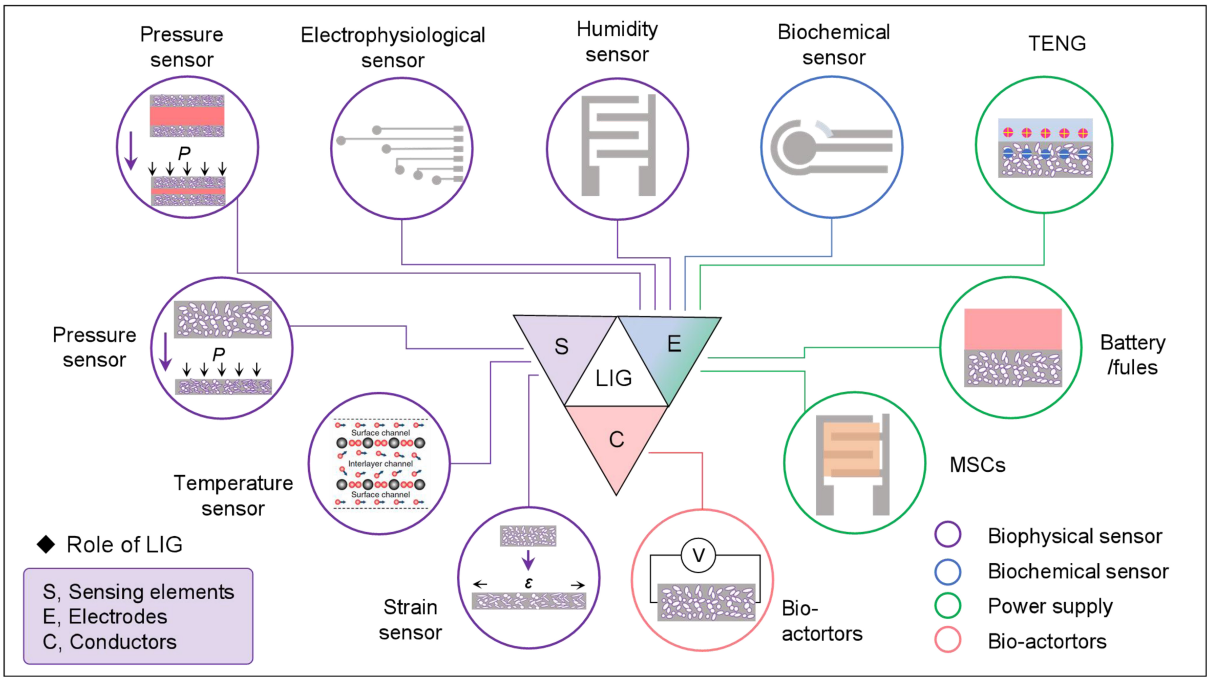

Figure 5. Schematic showcasing three leading roles of LIG playing in soft skin electronics. LIG: Laser-induced-graphene.

LIG with remarkable piezoresistive capability. The porous LIG materials can be directly utilized as sensing materials in soft skin electronics, including pressure, strain, and temperature sensors. The LIG-based pressure sensors can convert pressure stimuli into electrical resistance variations. The underlying working mechanism is briefly described as follows: the pressure stimulus decreases the interval between adjacent graphene interlayers, enlarging the contact area and reducing the electrical resistance. Various LIG-based pressure sensors with outstanding sensing performance have been developed for intelligent healthcare, such as pulse wave monitoring[60] and gait analysis[60]. In addition, engineers have fabricated strain sensors based on porous LIG for human health management, including joint movement detection[89], cardiovascular healthcare[3], *etc.* Under the external tensile stimulus, corresponding electrical resistance variations in LIG will occur. The distance between adjacent graphene interlayers was increased under strain stimuli, resulting in decreased contact area and increased electrical resistance. Additionally, elevated temperatures lead to increased electron-phonon scattering and thermal velocity of electrons within the sandwiched layers of LIG, ultimately leading to enhanced conductivity[90]. This character enables researchers to develop temperature sensors based on LIG[35,91].

Benefiting from its programmed conductivity and micromorphology, porous LIG is widely adopted as electrodes in soft skin electronics, including pressure, humidity, electrophysiological and biochemical sensors for bio-signals recording, triboelectric nanogenerators (TENGs) for energy harvesting, battery/biofuels for power supply, and micro-supercapacitors (MSCs) for energy storage. Due to the release of gaseous compounds during laser engraving, the LIG electrodes showcased porous structures with a high surface area of approximately 340 m^2/g[23]. These multiscale porous structures within LIG electrodes rendered biochemical sensors with remarkable sensing performance resulting from the large contact area between the chemical stimulus source and electrodes[75]. Meanwhile, engineers utilized LIG as conductors to develop various bio-actuators as effective interfaces for intelligent healthcare. Driven by specific voltage sources, the LIG-based device could realize thermal production[45], sound generation[46], designed deformations[32], *etc.* For example, Yang *et al.* reported a smart and wearable artificial throat (AT) based on

porous LIG, achieving speech recognition and generation to rehabilitate the patient's vocalization capability[46].

APPLICATIONS OF LIGS²E FOR INTELLIGENT HEALTHCARE

LIGS²E for biophysical signals detection

Physical signals detection

A densely interconnected 3D network of graphene flakes renders LIG with conductivity and excellent piezoresistive response capability. Motivated by this, engineers have designed LIGS²E to monitor biophysical signals. Kaidarova *et al.* developed a soft pressure sensor by laser-printing conductive porous graphene structure onto polyamide film packaged with an ultrathin coating material [Figure 6A][60]. The fabricated pressure sensor exhibited an outstanding sensitivity of 1.23 × 10^{-3} kPa, a low detection limit of approximately 10 Pa, a wide dynamic range (> 20 MPa), and excellent cycling stability (> 15,000 cycles). Profited by excellent mechanical sensing performance, the pressure sensors manage health when attached to the skin surface, such as heart rate monitor, gait analysis, and tactile perception. In addition, Luong *et al.* reported a 3D LIG foam printing process based on laminated object manufacturing [Figure 6B][36]. The fabrication process of the LIG foam is simple and low-cost: firstly, the PI layer with prepared LIG was stacked with one another using ethylene glycol as a binding agent; then the sandwiched layers were lased to fabricate macroscale LIG foams; finally, a fiber laser was utilized to mill the bulk LIG, forming LIG foams. The piezoresistive effect of the LIG foam was investigated by applying stress, which exhibited a significant gauge factor (GF) of approximately 40. In addition, the LIG foam presented an increased GF overuse while maintaining full stretchability. The developed pulse sensor based on LIG/PDMS precisely captured pulse waveforms from wrist arterial sites.

Learning from the bean pod structure, Tian *et al.* showcased a self-healable pressure sensor, which was composed of a polystyrene (PS) microspheres-based micro-spacer layer sandwiched between two laser-induced graphene/polyurethane (LIG/PU) sheets [Figure 6C][92]. The developed devices presented an outstanding sensitivity of 2,048 kPa^{-1}, a short response time of 16 ms, and self-healable performance. The sensors demonstrated several healthcare application scenarios, including human arterial pulse detection and gaits monitoring. Besides, a pressure sensor array (4 × 4) was fabricated, realizing a mapping of a two-dimensional spatial of pressure. Flexible pressure sensor arrays face an urgent challenge during practical applications, i.e., the realization of high spatial resolution and low crosstalk interference. To tackle this problem, Li *et al.* proposed a high-resolution pressure sensor array through a simple laser processing method, where the individual sensing elements were prepared by laser-induced graphitization and interconnects were created by laser-induced ablation to reduce crosstalk interferences [Figure 6D][93]. A 0.7 mm-resolution pressure sensor array validated that the crosstalk coefficient reduced from -8.21 to -43.63 dB. Besides, the individual sensing element inside the pressure sensor array presented a wide pressure working range of 80 kPa, a remarkable sensitivity of 1.37 kPa^{-1}, and a short response time of 20 ms.

In addition to compressive strain detection, the LIG functional materials are sensitive to tensile strain. Benefiting from this, engineers have developed various strain sensors based on LIG for healthcare. Carvalho *et al.* employed an UV laser to fabricate a flexible strain sensor, achieving a fourfold decrease in the penetration depth (5 μm). At the same time, the spatial resolution is doubled compared with the devices prepared by the typical IR source [Figure 6E][37]. The developed sensor showcased a mechanical sensitivity (GF) of approximately 20 in a 0%~1% strain range. Furthermore, when integrated into the skin surface, the sensor could detect radial and carotid pulse waves with detailed features. To increase the stretchability of the LIG/PI composites, researchers have attempted to prepare LIG on the PI/PDMS composites directly. For instance, Wang *et al.* employed a PDMS/PI composite substrate to fabricate LIG under the irradiation of an

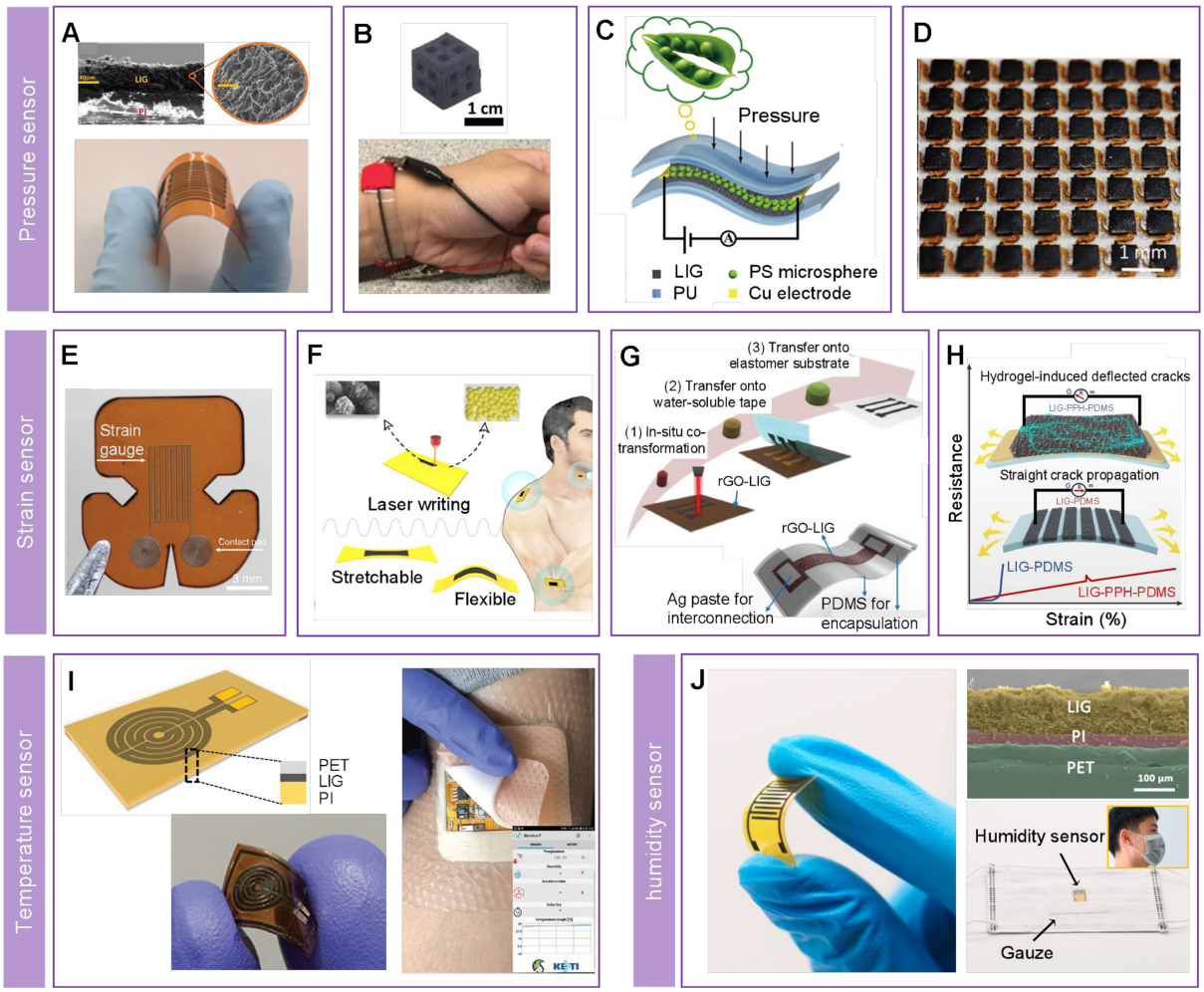

Figure 6. LIG-based biophysical skin electronics with single sensing mode for strain detection. (A) A LIG/PI-based flexible pressure sensor. Reproduced with permission[60]. Copyright 2020, WILEY-VCH; (B) A LIG foam-based soft pressure sensor. Reproduced with permission[36]. Copyright 2018, WILEY-VCH; (C) A LIG-based ultrasensitive pressure sensor inspired by bean pod structures. Reproduced with permission[92]. Copyright 2020, American Chemical Society; (D) A crosstalk-free and high-resolution soft pressure sensor array based on LIG. Reproduced with permission[93]. Copyright 2022, WILEY-VCH; (E) An optical photograph of a strain sensor based on LIG. Reproduced with permission[37]. Copyright 2018, WILEY-VCH; (F) A soft and stretchable strain sensor using LIG on PI/PDMS composites substrate. Reproduced with permission[81]. Copyright 2022, Springer Nature; (G) A LIG-based strain sensor using water-soluble tape-assisted transfer strategy. Reproduced with permission[89]. Copyright 2023, WILEY-VCH; (H) An ultrathin and stretchable LIG/hydrogel conductive composites prepared by cryogenically transferring process. Reproduced with permission[27]. Copyright 2023, Springer Nature; (I) A stable temperature sensor based on LIG for personal mobile monitoring. Reproduced with permission[35]. Copyright 2020, WILEY-VCH; (J) A flexible and wearable humidity sensor based on LIG. Reproduced with permission[38]. Copyright 2020, Elsevier B.V. LIG: Laser-induced-graphene; PI: polyimides; PDMS: polydimethylsiloxane.

IR laser beam [Figure 6F][81]. As expected, the developed device exhibited a wide strain detection range of over 15% and was able to match complex 3D shapes. In addition, three representative demonstrations, including wrist pulse monitoring, finger motion detection, and the tool of remote gesture control, validated that the proposed strain sensor had great potential for intelligent healthcare. To further increase the strain detection range, transferring LIG from a PI substrate into a rubber [such as PDMS, EcoFlex, polystyrene-block-poly(ethylene-ran-butylene)-block-polystyrene (SEBS), hydrogel, *etc.*] substrate is a practical approach. For example, Yoon *et al.* fabricated a conformal strain sensor through water-soluble tape (WST)-assisted transfer[89] [Figure 6G]. The reduced graphene oxide (rGO)-modified LIG was prepared by laser engraving a PI film modified with graphene oxide (GO). The WST-assisted transfer strategy, minimizing

the peel stress during the transfer process, could fabricate an ultrathin device. The fabricated ultrathin strain sensor (~30 μm in thickness) exhibited a high sensitivity of 2,425 (GF) in a wide strain range from 0% to 115%. Moreover, the developed sensor could monitor on-body strain and was suitable for broad, intelligent healthcare, including pulse wave monitoring, vocal sound detection, body movements perception, and translation of American sign language.

Meanwhile, to tackle the mechanical shortcomings in LIG's transfer process to elastomers, Lu *et al.* proposed a cryogenic transfer strategy (at -196 °C) with a super thin (thickness of 1.0-1.5 μm) and adhesive polyvinyl alcohol-phytic acid-honey (PPH) hydrogel[27] [Figure 6H]. The fast-cooling process could improve the interfacial binding strength between porous LIG and crystallized water inside the hydrogel. The interfacial PPH hydrogel layer could be an energy dissipation layer and out-of-plane conductive paths. There were electrically consistent deflected cracks in the developed LIG composites, resulting in an enhancement in stretchability from approximately 20% to 110%, with a further increase to approximately 220%.

Real-time monitoring of human temperature achieved by wearable soft skin electronics is vital in personalized mobile health monitoring. Based on the thermal response property of LIG, researchers have developed different kinds of soft temperature sensors[35,91,94]. For instance, as illustrated in Figure 6I, Gandla *et al.* reported a LIG-based soft temperature sensor featuring high stability and linearity, realizing real-time recording of skin temperature via the wireless platform for intelligent health management[35]. The proposed temperature sensor was a standalone system composed of LIG-based temperature, battery, signal processing circuits, and wireless modules that could be easily attached to human skin surfaces. The fabricated device showcased a negative temperature coefficient of resistance (TCR) of 0.00142 $°C^{-1}$ and stable performance even under complex environments. Benefiting from its excellent performance, the proposed temperature sensor can manage human health, such as breathing, touching with a finger, and blowing by mouth.

As a crucial physical indicator influencing our daily lives, humidity means the quantity of water in the atmosphere. It can be employed to monitor respiratory activities in a non-contact manner, facilitating the prevention and treatment of infectious respiratory diseases. Soft humidity sensors can be easily attached to curved surfaces, realizing various applications. The LIG has been widely utilized to develop humidity sensors because of the simple fabrication process, porous structures, good conductivity, and strong chemical stability[38,95,96]. For example, as illustrated in Figure 6J, Lan *et al.* reported a flexible and wearable humidity sensor based on a LIG-based interdigital electrode prepared by a laser direct engraving technology, which was convenient, effective, and robust[38]. Besides, due to unique 2D structures and super permeability to water molecules, GO was integrated as a humidity sensing element, which improved the humidity sensing performance of the device. The fabricated humidity sensor exhibited remarkable sensitivity [3,215.25 pF/% relative humidity (RH)], high stability (variations < ±1%), and low hysteresis. The noteworthy performance of the humidity sensor realized various applications, including non-contact humidity detection and human breath recording.

Electrophysiological monitoring

Benefiting from its electrical conductivity, the LIG can be used as a superficial electrode for electrophysiological signal recording, including electrocardiography (ECG) and electromyography (EMG). For instance, Dallinger *et al.* fabricated a LIG/MPU-based EMG sensor, which consisted of a pair of circular electrodes, connecting wires, and vertical interconnect access (VIA) for external wiring[34] [Figure 7A]. The developed EMG sensor was ultrathin, realizing outstanding conformal integration on the skin surface, excellent stretchability, and inelegant breathability. The subject wore the EMG sensor for three consecutive

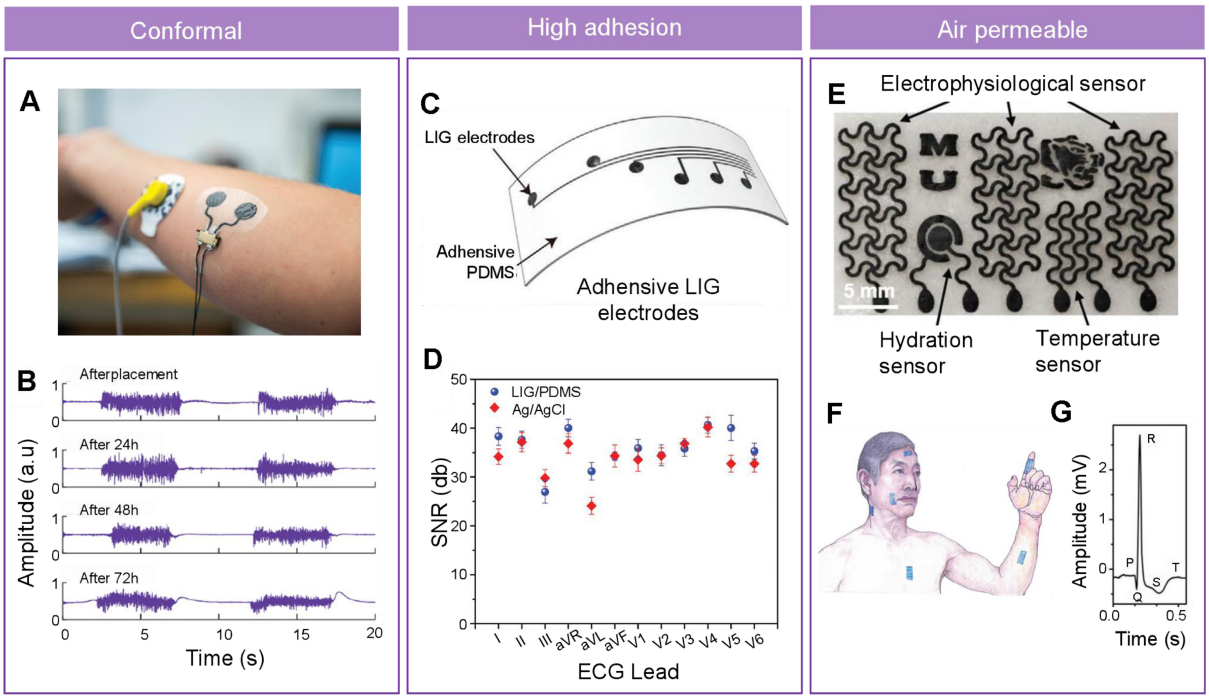

Figure 7. LIG-based biophysical skin electronics for electrophysiological monitoring. (A) Optical image of an ultrathin conformal LIG-based EMG sensor; (B) EMG recording results at different time points. Reproduced with permission[34]. Copyright 2020, American Chemical Society; (C) Schematic of adhesive LIG electrodes for ECG recording; (D) Comparison of SNR of ECGs captured by different type electrodes. Reproduced with permission[59]. Copyright 2021, WILEY-VCH Verlag GmbH & Co. KGaA, Weinheim; (E) Optical photograph of gas-permeable skin electronics containing electrophysiological, hydration, and temperature sensors; (F) Schematic for mounting the devices in the different positions to record various electrophysiological activities; (G) Enlarged ECG signals illustrate clear features. Reproduced with permission[83]. Copyright 2018, WILEY-VCH Verlag GmbH & Co. KGaA, Weinheim. LIG: Laser-induced-graphene; EMG: electromyography; ECG: electrocardiography; SNR: signal-to-noise ratio.

days while maintaining normal daily activities, including work, exercise, showering, and sleep. It was evident that there was only a small variation in signal quality in the recorded EMG signals [Figure 7B].

In addition to conformal attachment, the robust bonding strength between LIG and the substrates, enabling it to resist abrasion and washing, is crucial for long-term wearability and monitoring in daily life. Yang *et al.* proposed dry electrodes LIG/PDMS composites, achieving flexible, durable, and high performance[59]. A PDMS/ethoxylated polyethylenimine (PEIE) mixture was coated on the region outside LIG, achieving a single-sided adhesive epidermal electrode [Figure 7C]. The results revealed that the fabricated LIG/PDMS dry electrodes exhibited high electrical performance and excellent robustness after high-intensitive mechanical treatments (bending tests: > 10,000 cycles; high-power ultrasonic treatments: 5 h), showcasing great potential for long-term monitoring. Furthermore, they fabricated an integrated staff-shaped chest electrode for 12-lead ECG monitoring, which exhibited excellent performance rivaling commercial Ag/AgCl electrodes [Figure 7D].

Most existing skin electronics exhibit restricted air permeability, impeding the evaporation of sweat and consequently limiting their long-term feasibility. Sun *et al.* reported an effective approach for fabricating breathable skin electronics, utilizing porous LIG and silicone elastomer sponges [Figure 7E][83]. The fabricated devices exhibited remarkable water-vapor permeability (~18 $mg \cdot cm^{-2} \cdot h^{-1}$), approximately 18 times higher than the silicone films without pore structures. The developed sensors were soft and flexible and could be attached to different skin surfaces to collect signals [Figure 7F]. For instance, the device collected

Table 1. Summary of typical LIG-based single-mode biophysical sensors for healthcare

LIG composites (role)/substrate	Signals	Sensitivity	Working range	Ref.
LIG (S)/PI	Pressure	1.23×10^{-3}	0-20 MPa	[60]
LIG foam (S)/PDMS	Pressure	GF: 40	0%-20%	[36]
LIG (S)/PS@PU	Pressure	2,048 kPa^{-1}	0-100 kPa	[38]
LIG (S)/PI	Pressure	1.37 kPa^{-1}	0-80 kPa	[93]
LIG/PI	Strain	GF: 20	0%-1%	[37]
LIG/PI	Strain	GF: 14.1	0%-1.2%	[84]
LIG/PI	Strain	GF: 11.2	0%-1.4%	[77]
LIG/PI	Strain	GF: 112	0%-1.5%	[85]
LIG/PI	Strain	GF: 40	0%-0.25%	[42]
LIG/PI	Strain	GF: 316.3	0%-10%	[44]
LIG/PI-PDMS	Strain	GF: 75	0%-10%	[81]
LIG/PSPI-PDMS	Strain	GF: 380	0%-120%	[82]
LIG/PI/Ecoflex	Strain	GF: ~1.3	0%-135%	[41]
LIG/PDMS	Strain	GF: 2,336	0%-3%	[3]
Graphene/PVA	Strain	GF: 1.33	0%-4%	[86]
LIG/PDMS	Strain	GF: 950	0%-30%	[45]
LIG/PDMS	Strain	GF: 160	0%-30%	[87]
LIG/PDMS sponge	Strain	GF: 1.3	0%-60%	[83]
	Strain	GF: 0.006	0%-1,000%	
LIG/PDMS	Strain	GF: 2,212.5	0%-65%	[58]
LIG/PDMS	Strain	GF: 5	0%-100%	[68]
MXene@EDOT/LIG-SEBS	Strain	GF: 2,075	0%-27%	[74]
LIG/Ecoflex	Strain	GF: 114.8	0%-50%	[88]
rGO-LIG/Ecoflex	Strain	GF: 2,425	0%-115%	[89]
LIG/MPU	Strain	GF: 40	0%-100%	[34]
LIG/PPH/PDMS	Strain	GF: 30	0%-220%	[27]
LIG/PI	Temperature	0.00142 $°C^{-1}$	-10-60 °C	[35]
LIG/paper	Temperature	-2.8×10^{-3} °C	10-60 °C	[91]
LIG/PI	Temperature	0.0011 $°C^{-1}$	20-60 °C	[94]
LIG (E)/PI	Humidity	3,215.25 pF/% RH	10%-90% RH	[38]
LIG (E)/PEEK	Humidity	1,700 kΩ/% RH	11%-97% RH	[95]
LIG (E)/PI	Humidity	28,231-fold increase in current	26.1%-90.2% RH	[96]
LIG (E)/MPU	EMG	10-30 dB	-	[34]
LIG (E)/PEIE-PDMS	ECG	>30 dB	-	[59]
LIG (E)/PDMS sponge	ECG	~21.6 dB	-	[83]

LIG: Laser-induced-graphene; PI: polyimides; PDMS: polydimethylsiloxane; GF: gauge factor; PS: Polystyrene; PU: polyurethane; PSPI: photosensitive polyimides; PVA: polyvinyl alcohol; EDOT: 3, 4-ethylene dioxythiophene; SEBS: polystyrene-block-poly(ethylene-ran-butylene)-block-polystyrene; rGO: reduced graphene oxide; MPU: medical polyurethane film; PPH: polyvinyl alcohol-phytic acid-honey; RH: relative humidity; PEEK: poly (ether ether ketone); EMG: electromyography; PEIE: ethoxylated polyethylenimine; ECG: electrocardiography.

high-quality ECG signals when adhered to the human skin surface, which were quantitatively comparable to those recorded with the conventional Ag/AgCl gel electrodes. The magnified ECG signals exhibited visible P-wave, QRS complex, and T-wave [Figure 7G], validating the proposed device's high performance. Typical LIG-based single-mode biophysical sensors for healthcare are summarized in Table 1.

LIG-based skin electronics for multiple biophysical signals detection

Multiple biophysical signal collection can increase the diagnostic accuracy of healthy status. Motivated by this objective, researchers have further attempted to develop various multimodal $LIGS^2E$ for multiple

biophysical signals collection and intelligent healthcare. Chen *et al.* reported a high-performance porous LIG composites-based sensor for strain and temperature detection fabricated by a simple laser process[58] [Figure 8A]. The developed dual-mode sensor showcased a remarkable strain sensitivity (GF: 2,212.5) in a wide linear range of 0%-65%, ultralow detection limit (< 0.0167%), and temperature sensitivity of 0.97×10^{-2} °C^{-1} in a broad linear range of 10-185 °C. Owing to this high performance, the proposed dual-mode sensor could simultaneously record the heat stress and human pulse waves when integrated into the wrist skin surface [Figure 8B].

To track the sleeping status of vulnerable populations, Xu *et al.* exhibited a wireless sensing patch based on LIG, which could detect multimodal indicators (sleeping postures, respiration rate, and diaper moisture) and feedback alarms[97] [Figure 8C]. In this study, the LIG was utilized as active porous sensing materials in strain sensors for respiration rate detection and was employed as highly conductive electrodes in tilt and humidity sensors for sleeping postures and diaper moisture perception, respectively. The tilt sensor was created by confining a GaInSn (Galinstan) droplet within a cavity integrated with patterned LIG electrodes, achieving the perception of 18 slanting directions. Originating from the various slanting orientations, the contact and separation between the liquid metal droplets and conductive LIG electrodes determine the "ON" and "OFF" states. As a proof-of-concept, a volunteer wore an intelligent diaper integrated with the proposed multimodal sensor device with feedback tracking functions, achieving real-time monitoring of sleeping posture, respiration, and wetness.

Similarly, Babatain *et al.* reported fully standalone LIG-based multifunctional skin electronics for multiple parameters (inertial, temperature, humidity, and breathing) detection[98] [Figure 8D]. The proposed inertial sensor comprised graphene-coated liquid metal droplets and 3D circular channels. This creative design rendered an inertial sensor with an excellent sensitivity of 6.52% $m^{-1} \cdot s^2$ in a wide range (1-30 m/s^2) and outstanding stability (> 12,500 cycles). After integrating optimized multifunctional sensors with a wireless programmable system on a programmable system on a chip (PSoC) signal processing circuit, a fully standalone platform was created, which achieved monitoring of human healthcare and soft human-machine interfaces in a real-time manner.

Electronic gloves (e-gloves) integrated with multifunctional sensing capabilities can render robotic/prosthetic hands with excellent perception performance to feel the physical aspects of the real world. Sharma *et al.* reported an all-directional strain-insensitive e-glove through laser engraving techniques, realizing real-time pressure monitoring, temperature, humidity, and ECG signals [Figure 8E][72]. To avoid the influence of external stretch on the performance of e-gloves, the sensing area and interconnections were designed as ripple-like meandering patterns. In addition, the crosslinking network of the CNT in the porous LIG could reduce the stress effect. The developed e-glove could simultaneously assess the temperature and humidity of objects, pressure profile on the fingers, ECG signals, hand movements, and gestures, exhibiting great potential application in prosthetic hands.

Although various multifunctional skin electronics have been fabricated, seamlessly integrating multiple functional sensors into a common stretchable substrate without interfering remains challenging. To overcome this shortcoming, Zhang *et al.* developed a multifunctional soft skin electronic system by integrating strain, temperature, and ECG sensors into a stretchable and soft SEBS substrate without interfering with each other [Figure 8F][74]. The heterogeneity of these three different sensors was enabled by electrophoretically depositing MXene-Ti_3C_2Tx@EDOT onto porous LIG, forming LIG/MXene-Ti_3C_2Tx@EDOT composites. As expected, the fabricated device successfully exhibited synchronous strain, temperature, and ECG detection.

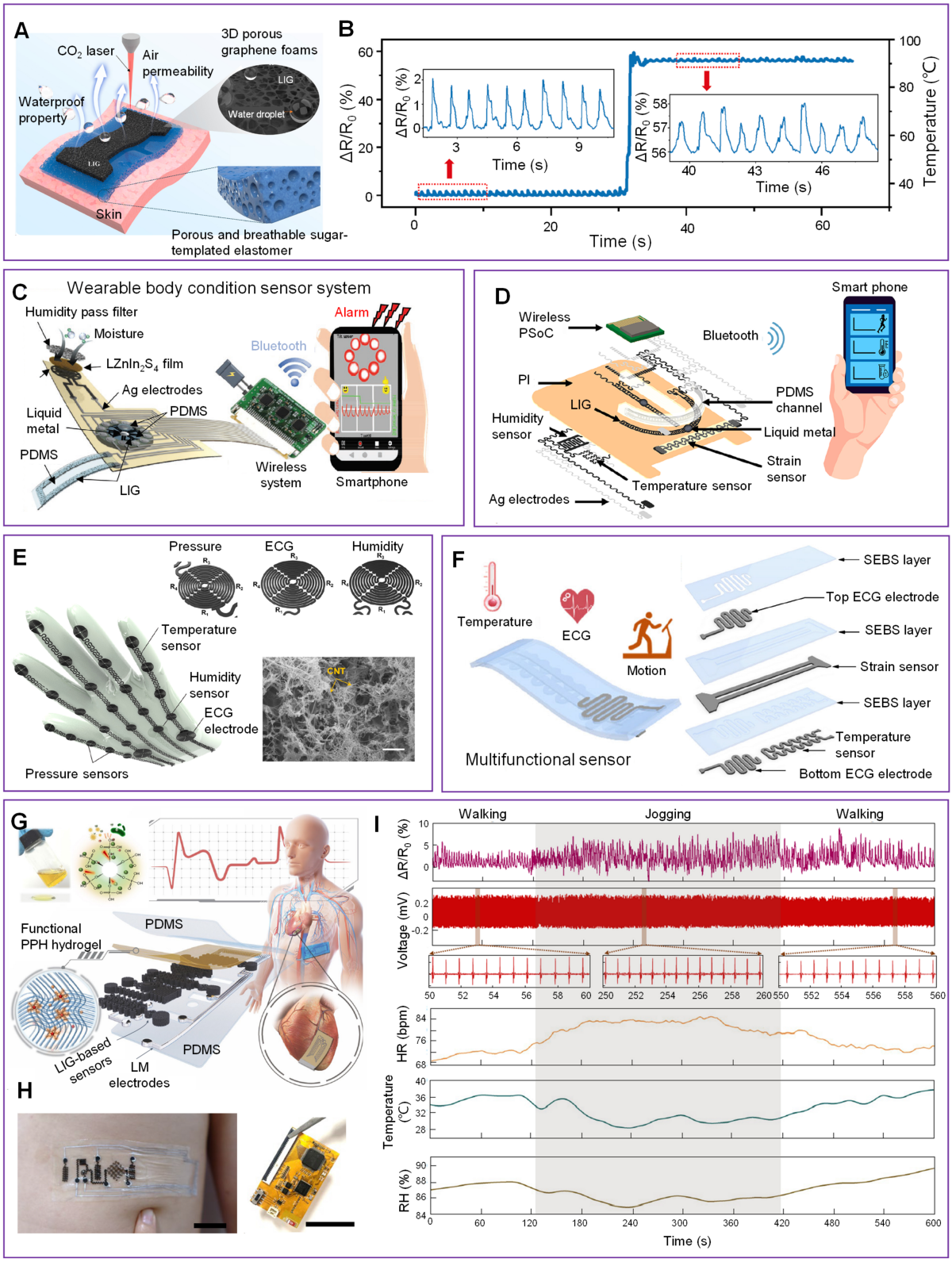

Figure 8. LIG-based biophysical skin electronics with multiple sensing modes for healthcare. (A) Schematic illustrating the structure and preparation of LIG-based dual-mode sensors; (B) Simultaneous monitoring of skin temperature and pulse waves. Reproduced with permission[58]. Copyright 2022, Elsevier B.V.; (C) Schematic of a wireless multimodal sensor system integrated with tilt, breath, and moisture sensors for body condition monitoring. Reproduced with permission[97]. Copyright 2021, Wiley-VCH GmbH; (D) Schematic

illustrating a multifunctional wireless platform with different layers of inertial, temperature, humidity, and breathing sensors. Reproduced with permission[98]. Copyright 2022, American Chemical Society; (E) Schematic diagram of an electric glove integrated with pressure, temperature, ECG, and humidity sensors. Reproduced with permission[72]. Copyright 2023, American Chemical Society; (F) Schematic illustrating layered structures of multifunctional sensors. Reproduced with permission[74]. Copyright 2022, Springer Nature; (G) Illustration of stretchable LIG/hydrogel-based multifunctional wearable electronics; (H) An optical image of developed LIG-based sensing multimodal; (I) Real-time synchronous monitoring of typical five indicators at normal, walking, and jogging states. Reproduced with permission[27]. Copyright 2023, Springer Nature. LIG: Laser-induced-graphene; ECG: electrocardiography.

They benefited from conformal features; ultrathin multifunctional skin electronics achieve the perfect balance between sensing performance and user comfort level. As mentioned above, Lu *et al.* proposed a creative strategy, termed the cryogenic transfer approach, completing the transfer of LIG onto ultrathin (~11 μm in thickness) PPH/PDMS substrate[27]. They designed a stretchable and soft skin-integrated sensing patch to collect biophysical signals containing mechanical, temperature, humidity, and ECG [Figure 8G and H]. A standalone multimodal skin electronics system was established by integrating the fabricated soft sensor system with a flexible printed circuit board (fPCB) for signal processing and transmission. Five indicators, including respiration rate, ECG, heart rate, skin temperature and humidity, were collected from the volunteer performing three activities (baseline, walking, and jogging) [Figure 8I]. As expected, all these five detected indicators reflected the corresponding health status. It was clear that this multimodal skin electronics system offered a viable prediagnostic strategy for intelligent healthcare monitoring. Typical LIG-based multimodal biophysical sensors for healthcare are summarized in Table 2.

Machine learning-assisted LIGS²E

The fast development of machine learning benefits the design and fabrication of flexible electronics, facilitates signal processing, and improves system performance[99,100]. Lu *et al.* developed a TENG-based soft tactile sensor system, where machine learning was employed to guide the design, including output signals selection and fabrication parameters[101]. The proposed tactile sensor consisted of four layers, i.e., top and bottom PDMS encapsulations, porous LIG-based interdigital electrodes, and a Fluorinated ethylene propylene (FEP) film [Figure 9A]. Its working mechanism was described as follows: When the human finger touched the PDMS surface, the skin was positively charged, originating from their different electron affinities. Following this, horizontal sliding of the charged finger will generate electron transfer between the LIG electrodes, originating from the electrostatic induction principle [Figure 9B]. With the assistance of machine learning for six contact modalities analysis, the parameter values of the output signals, the distribution density of LIG electrodes, and diverse surface microstructures were optimized. The developed tactile sensor with optimal sensing performance could precisely distinguish ten braille numbers with a high accuracy of 96.12% by utilizing a customized convolutional neural network (CNN) model [Figure 9C].

Meanwhile, Xie *et al.* proposed a machine learning-assisted soft pressure sensor based on LIG to realize real-time tactile perception and voice recognition [Figure 9D][102]. The intelligent pressure sensor integrated with a triboelectric layer converted pressure stimulus into electrical signals, benefiting from the contact electrification effect. Due to its softness and high performance, the developed intelligent pressure sensor could be attached to a facemask to collect signal outputs that responded to the volunteer's speaking. The intelligent pressure sensor could recognize distinct voices when the speaker pronounced three different sentences: "How do you do?", "Nice to meet you", and "See you later" [Figure 9E]. With the help of machine learning, the intelligent pressure sensor could accurately classify various voices, achieving a high accuracy of approximately 94.6% [Figure 9F].

The soft pulse sensor exhibits great potential for real-time monitoring and intelligent management of cardiovascular health. Most existing soft pulse sensors have limitations, including high cost, clinical

Table 2. Summary of typical LIG-based multimodal biophysical sensors for healthcare

LIG composites (role)/substrate	Signals	Sensitivity	Intelligent applications	Ref.
LIG (S)/PDMS foam	Strain; temperature	GF: 2,212.5; TCR: 0.97 × 10^{-2} °C^{-1}	Simultaneously record heat stress and pulse waves	[58]
LIG (S, E)/PDMS	Tilt; strain; humidity	GF: ~10; humidity: -0.667/%	Sleeping safety monitoring for vulnerable populations (e.g., elderly, infants, disabled)	[97]
LIG (S, E)/PI	Inertial; temperature; humidity; breath rate	I: 6.52% m^{-1}·s^{2}; TCR: 215.2 m·Ω·°C^{-1}	Monitoring of human physical and health activities, legged-robot activities, and the control of the robotic arm via a human	[98]
LIG/CNT (S, E)/SEBS	Pressure; temperature; humidity; ECG	P: 0.506 kPa^{-1}; TCR: 0.212% °C^{-1}; H: 0.053%/%; ECG: 35 ± 3 dB	Simultaneously assess the temperature and humidity of an object, pressure distribution on the fingers, ECG signals, hand movements, and gestures	[72]
MXene-Ti_3C_2Tx@EDOT @LIG (S, E)/SEBS	Strain; temperature; ECG	S: 2,075; TCR: 0.86%; ECG: 20.14 dB	Simultaneous measurement of strain, temperature, and ECG	[74]
LIG (S, E)/PPH/PDMS	Mechanical; temperature; humidity; ECG	M: 30; TCR: 0.35% °C^{-1}; H: 0.81%/%	5 detected indicators reflected the corresponding health status during movements	[27]

LIG: Laser-induced-graphene; PDMS: polydimethylsiloxane; GF: gauge factor; TCR: temperature coefficient of resistance; PI: polyimides; CNT: carbon nanotubes; SEBS: polystyrene-block-poly(ethylene-ran-butylene)-block-polystyrene; ECG: electrocardiography; EDOT: 3, 4-ethylene dioxythiophene; PPH: polyvinyl alcohol-phytic acid-honey.

validation, and real-time cardiovascular disease (CVD) events diagnostics, which hinder their population-wide practical applications. To tackle this challenge, Ma *et al.* reported a cheap, clinically validated, smart, and soft pulse monitoring system (termed FlexiPulse) based on porous LIG for CVD management and diagnostics[3]. The ultrathin FlexiPulse can conform to the skin surface [Figure 9G]. The FlexiPulse was highly sensitive to deform with the pulse waves when adhered to the epidermis above the artery [Figure 9H]. The developed intelligent pulse sensor exhibited a high sensitivity of 2,336, an extreme-low strain detection limit of 0.0056%, excellent stability (> 24,000 cycles), and clinical accuracy (> 93%). Integrated with machine learning, the FlexiPulse realized clinical evaluation of actual CVD events [containing atrial fibrillation (AF) and atrial septal defect (ASD)] with a high accuracy of approximately 98.7% [Figure 9I]. Typical machine learning-assisted soft biophysical sensors based on LIG for intelligent healthcare are summarized in Table 3.

LIGS²E for biochemical signals detection

Biochemical signals detection

The porous structures endow LIG electrodes with large contact areas with surrounding chemical stimuli, resulting in high performance in biochemical sensors[75]. Rahimi *et al.* demonstrated a stretchable electrochemical pH sensor consisting of a pH-sensitive working electrode and a liquid-junction-free reference electrode for wearable healthcare applications [Figure 10A][41]. The electrodes were developed by bonding LIG/PI composites to soft Ecoflex substrates. The porous LIG electrodes were modified with PANI, which functioned as the conductive filler and pH-sensitive film. Meanwhile, introducing serpentine patterned interconnections rendered the pH sensor with excellent stretchability, which withstood elongations of up to 135%. The experimental results validated that the developed pH sensor presented a linear -53 mV/pH sensitivity in a pH 4-10 physiological range. The sensing performance remained stable even under a tensile strain of 100% [Figure 10B].

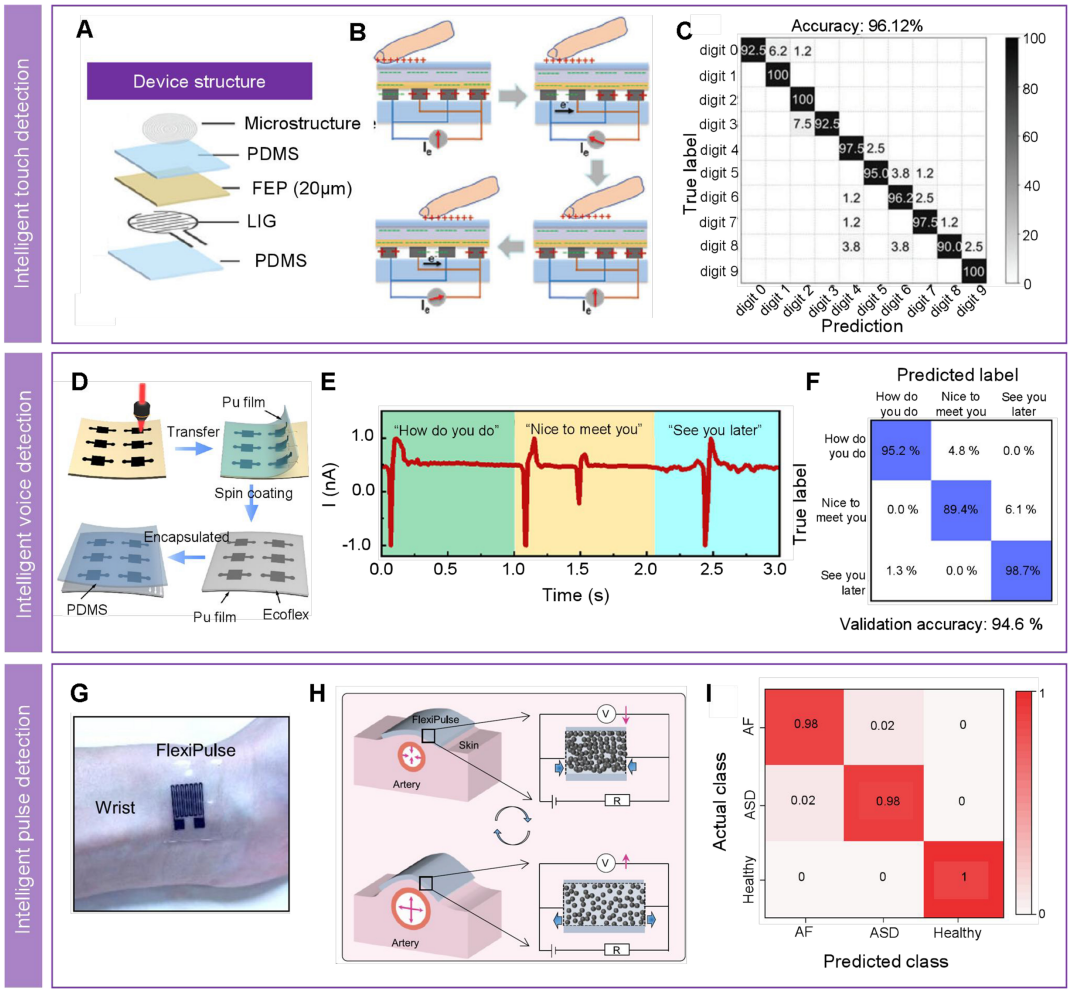

Figure 9. Machine learning-assisted LIG-based biophysical skin electronics for intelligent healthcare. (A) Schematic illustrating the structure of LIG-based TENG tactile sensor; (B) Working principles of the tactile sensor; (C) Classification results of ten braille numbers. Reproduced with permission[101]. Copyright 2023, Wiley-VCH GmbH; (D) Illustration of the fabrication process of the self-powered flexible sensor; (E) Current outputs of flexible pressure sensor while speaking three different sentences; (F) Confusion matrix of the machine learning outcome. Reproduced with permission[102]. Copyright 2023, American Chemical Society; (G) Optical photograph of intelligent pulse sensor attached on wrist arterial site; (H) Working mechanism of the intelligent pulse sensor; (I) Classification results of three different CVD events. Reproduced with permission[3]. Copyright 2023, Cell Press. LIG: Laser-induced-graphene; TENG: triboelectric nanogenerator; CVD: cardiovascular disease.

As a conducting polymer, PEDOT exhibited several advantages, including high electrical conductivity, low oxidation potential, remarkable electrochemical activity, outstanding stability, and splendid biocompatibility. It often was deposited with highly porous, fractal-type microstructures with large surface areas. Xu *et al.* developed a highly selective electrochemical sensor based on a PEDOT-modified LIG electrode for dopamine (DA) detection [Figure 10C][75]. The electrodeposition of PEDOT onto the porous LIG electrodes resulted in the formation of PEDOT@LIG electrodes, which exhibited a 3D porous morphology characterized by a larger surface area and roughness compared to the parent LIG electrodes. Due to enhanced electron transfer responses, PEDOT electrodes are valuable in electrochemical sensors. As expected, the PEDOT@LIG sensor showcased a noteworthy performance improvement compared to parent LIG electrodes [Figure 10D].

Table 3. Summary of machine learning-assisted soft biophysical sensors based on LIG for intelligent healthcare

LIG composites (role/substrate	Signals	Performance	Intelligent applications	Ref.
LIG (E)/PDMS	Pressure	NA	Distinguish ten braille numbers with a high accuracy of 96.12%	[101]
LIG (E)/PU	Pressure	Sensitivity: 0.05 kPa^{-1}; stability: 1,000 cycles	Classify various voices with a high accuracy of 94.6%	[102]
LIG (S)/PDMS	Strain	GF: 2,336; limit: 0.0056%; clinical accuracy: >93%	Clinical evaluation of actual CVD events, high accuracy of 98.7%	[3]

LIG: Laser-induced-graphene; PDMS: polydimethylsiloxane; PU: polyurethane; GF: gauge factor; CVD: cardiovascular disease.

Meanwhile, Zhu *et al.* reported a soft non-enzymatic glucose sensor based on LIG-electrodes coated with a uniform metal (Ni or Ni/Au), which was packaged by a porous encapsulating reaction cavity for wearable applications [Figure 10E][40]. As expected, the fabricated glucose sensor based on LIG foams exhibited a high sensitivity of 1,080 $\mu A \cdot mM^{-1} \cdot cm^{-2}$, whereas the device with LIG fibers enhanced the detection sensitivity up to 3,500 $\mu A \cdot mM^{-1} \cdot cm^{-2}$. Then, they attached the developed glucose sensor onto the arm surface to evaluate its on-body performance. The results illustrated that the proposed glucose sensor could monitor the variations in glucose concentration in sweat, i.e., decreased from 0.26 to 0.15 mM, responding to 1 and 3 h after lunch [Figure 10F].

Zhao *et al.* reported an iron nano-catalysts (FeNCs)/LIG-based wearable electrochemical patch, where FeNCs functioned as the catalyst and LIG was utilized as the signal-improving substrate [Figure 10G][103]. A two-channel hydrogel chip was integrated with FeNCs/LIG to implement the wearable configuration. Profited from the unique 3D microstructures of LIG and the remarkable electrocatalytic activity of FeNCs, the wearable electrochemical patch exhibited outstanding sensing performance for sweat metabolites [tyrosine (Tyr) and uric acid (UA)] detection. When mounted onto a human skin surface, the device could accurately monitor Tyr and UA in sweat, essential in non-invasive health monitoring and management. The results exhibited that the concentrations of Tyr evaluated by the skin-integrated patch were comparable to those assessed by the liquid chromatography-mass spectrometry (LC-MS), illustrating good reliability [Figure 10H].

Torrente-Rodríguez *et al.* reported a standalone wireless health management device, termed a graphene-based sweat stress monitoring system (GS4), to explore the dynamics of the sweat stress hormone [Figure 10I][43]. Combining LIG and immunosensing approaches effectively detected cortisol in human sweat and saliva. In addition, the GS4 device was attached to the skin surface to analyze sweat cortisol during a 50-minute stationary cycling exercise. The results revealed that the sweat cortisol increased and reached the highest level after continuous biking [Figure 10J]. This soft and wearable point-of-care device provided a practical approach for stress monitoring and continuous evaluation of the psychological states of subjects.

In addition to biofluids, the exhaled gas carries essential information for disease diagnostics. For instance, exhaled NOx is a crucial biomarker for human respiratory disease diagnostics[104-106]. Motivated by this, Yang *et al.* developed a moisture-resistant and stretchable NOx gas sensor based on porous LIG, where the LIG sensing/electrode region was sandwiched between a semipermeable PDMS film and a soft elastomeric substrate for patient breath analysis [Figure 10K][39]. The gas sensor fabricated with optimized processing parameters showcased excellent performance: significant sensitivity of 4.18‰ ppm^{-1} to NO and 6.66‰ ppm^{-1} to NO_2, and ultralow detection limit of 8.3 ppb to NO and 4.0 ppb to NO_2. The introduction of a LIG electrode with a serpentine pattern and strain isolation from the PI island enabled the gas sensor to undergo

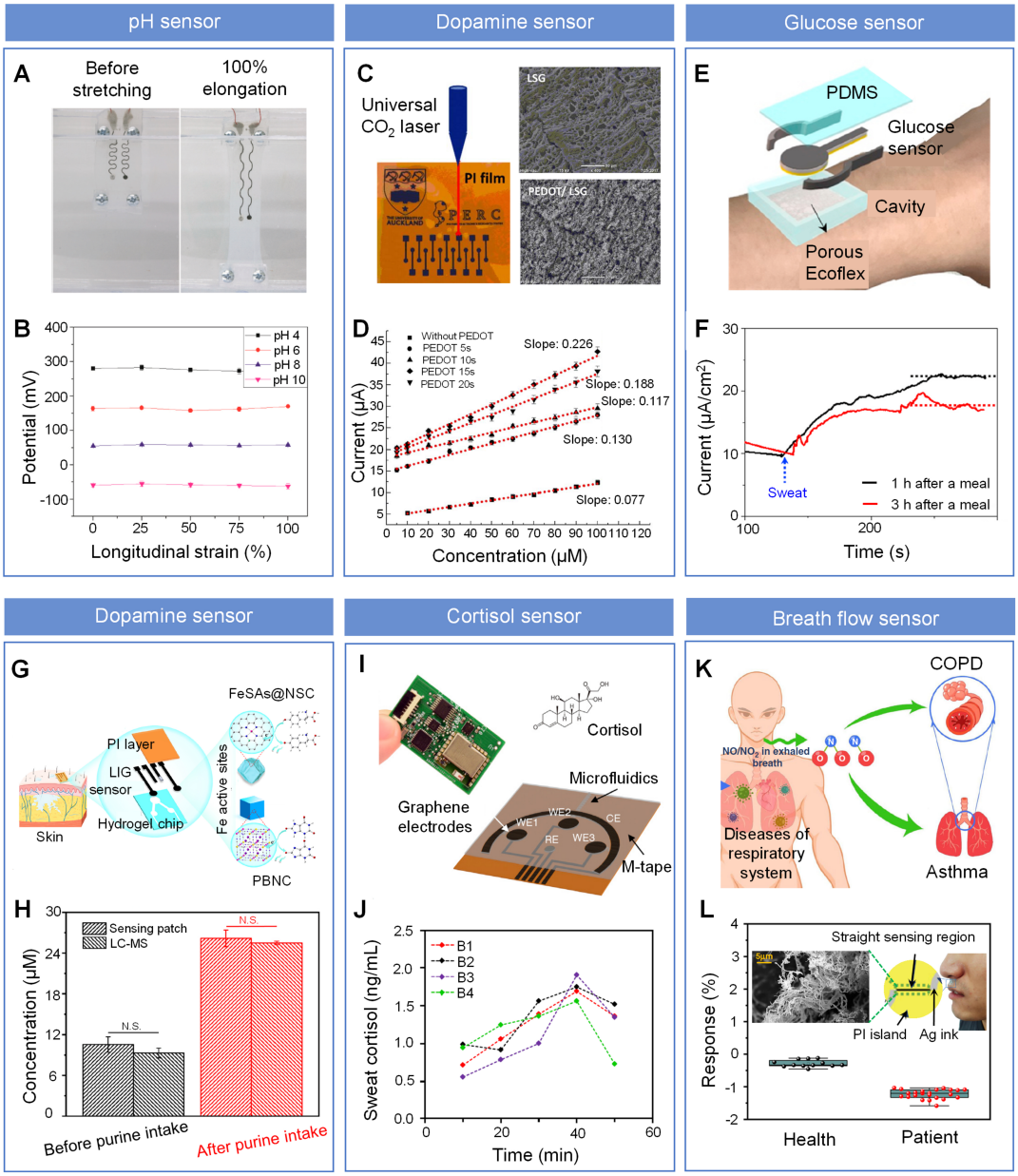

Figure 10. LIG-based biochemical skin electronics with single sensing mode for intelligent healthcare. (A) Optical photograph of pH sensor under longitudinal strain; (B) Outputs of a pH sensor responding to different transverse strains. Reproduced with permission[41]. Copyright 2017, American Chemical Society; (C) An electrochemical dopamine sensor based on PEDOT-modified LIG; (D) Response of electrochemical dopamine sensor to different concentrations of dopamine. Reproduced with permission[75].Copyright 2018, Elsevier B.V.; (E) Illustration of a packaged wearable non-enzymatic glucose sensor; (F) Experimental results of the glucose sensor, responding to human sweats at different time points. Reproduced with permission[40].Copyright 2021, Elsevier B.V.; (G) Schematic of wearable FeNCs/LIG-based electrochemical patch for sweat metabolites monitoring; (H) Tyr concentrations evaluated by developed electrochemical patch and LC-MS. Reproduced with permission[103].Copyright 2024, Elsevier B.V.; (I) A soft electrochemical sensing patch for cortisol detection; (J) Cortisol monitoring from three physically untrained volunteers (B1, B2, B3) and one trained volunteer (B4) in a cycling exercise. Reproduced with permission[43].Copyright 2020, Cell Press; (K) Schematic illustration exhibits the use of NOx gas as a promising biomarker for representative human diseases; (L) Response of the gas sensor to human exhaled breath samples from different subjects, including patients (with respiratory diseases) and healthy volunteers. Reproduced with permission[39]. Copyright 2022, Springer Nature. LIG: Laser-induced-graphene; PEDOT: poly(3,4-ethylenedioxythiophene); FeNCs: iron nano-catalysts; Tyr: tyrosine; LC-MS: liquid chromatography-mass spectrometry.

a uniaxial tensile strain of 30%. The human experiments showed that the developed gas sensors could

precisely classify respiratory disease patients from healthy human subjects by analyzing clinical breath samples [Figure 10L].

LIG-based skin electronics for multiple biochemical signals detection

Multiple biochemical signals recording or incorporating biochemical information with biophysical information could enhance the device's performance for intelligent healthcare. Yang *et al.* reported an entirely laser-engraved sensing system, which contained LIG-based physical sensors for temperature and respiration rate monitoring, a highly sensitive chemical sensor based on LIG for low concentrations of UA and Tyr detection, and a laser-fabricated chip for dynamic sweat collection[42]. The sensing system was composed of five layers, i.e., multimodal sensors prepared on a flexible PI film, microfluidic channels engraved on a double-sided medical adhesive layer, and inlet-patterned polyethylene terephthalate (PET) layer, and a medical adhesive layer. When the sweat flowed into the sensing system, the LIG-CS monitored sweat UA and Tyr and LIG-PS evaluated the temperature and strain-related physiological signals [Figure 11A and B]. As expected, the fully standalone sensing system could be attached to different human body parts, the signals of which were displayed on a mobile terminal [Figure 11C]. The high performance enabled this sensing system to monitor the variations in sweat UA and Tyr, skin temperature and respiration rate, responding to cycling exercise experienced by a healthy individual [Figure 11D]. A noticeable decrease in UA and Tyr concentrations was probably due to profuse sweat secretion. Wang *et al.* exhibited a wearable multifunctional skin electronics system based on porous LIG and double-side configurations, which enabled avoiding signal interferences among different modal modules [Figure 11E][107]. This wearable system could simultaneously record various physiological signals, including electrophysiological signals (such as ECG, EMG, *etc.*), mechanical signals (i.e., strain, pressure, temperature, proximity, *etc.*), and concentration variations of various biochemical signals containing sodium ion (Na^+), hydrogen ion (H^+), acetone gas, and nitrogen dioxide (NO_2). Besides, it could produce and store energy through integrated energy harvesters and storage units. The experimental results showcased that the fabricated device could precisely monitor the physiological status variations in subjects caused by exercise, including body temperature fluctuations, Na^+ concentration increase, and rapid breathing and heartbeat [Figure 11F and G]. Typical LIG-based biochemical sensors for healthcare are summarized in Table 4.

LIGS^{2}E as bio-actuators

Besides biosensors, the LIG facilitates the development of bio-actuators as an interface for further stimulus generation (for instance, sound, heat, *etc.*) and healthcare. Most existing soft skin electronics focus on the monitoring of physiological signals without the capability of sounding an alarm. Developing self-alarm health management devices integrated with two functions of physiological signals monitoring and sound alarm synchronously could further improve intelligent healthcare. Chen *et al.* showcased a LIG-based dual functional electric skin (E-skin) for simultaneous real-time health monitoring and alarm [Figure 12A][44]. The developed E-skin with shutter pattern achieved excellent overall performance, with a GF of 316.3, capable of detecting various physiological indicators, such as respiration monitoring, voice recognition, and wrist pulse perception. Meanwhile, the fabricated shutter-patterned E-skin could sound an alarm at 200 Hz to 20 kHz in a broadband frequency. Benefiting from its outstanding mechanical and acoustic performance, the E-skin exhibited wide applications in health monitoring and alarm of diseases, for instance, sleep apnea [Figure 12B].

In addition, Huang *et al.* demonstrated a soft multifunctional (detection and warning) sensing patch, utilizing mechanical and thermal effects of LIGs [Figure 12C][45]. The strain sensor with a mesh pattern exhibited a mechanical sensitivity of up to 950 (GF), which could detect human motions and monitor weak physiological signals, such as pulse waves. The prepared heater without patterned LIG exhibited better heating performance than the device with a mesh pattern. Then, the developed device was integrated into

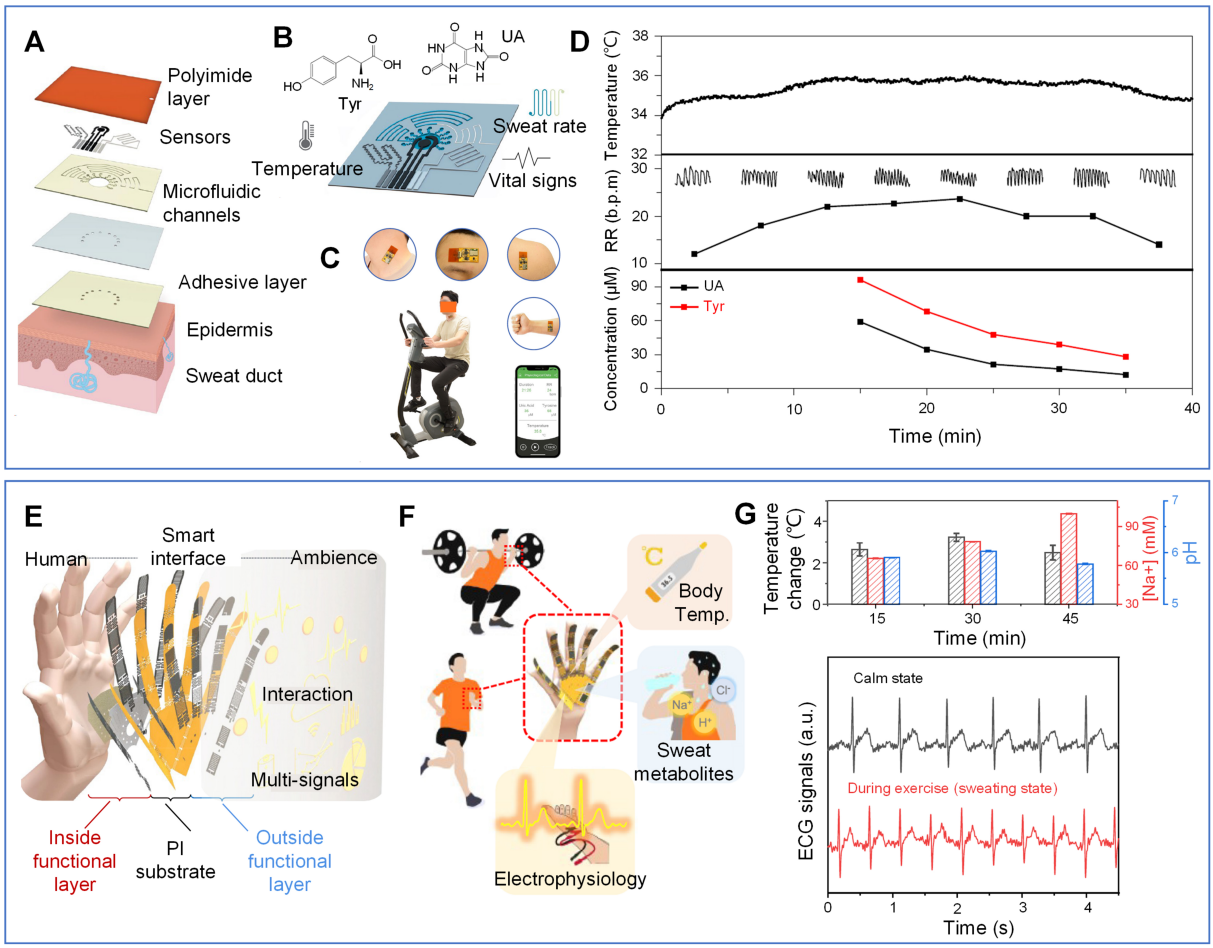

Figure 11. LIG-based biochemical skin electronics with multiple sensing modes for intelligent healthcare. (A) Layered view of the sensor structure; (B) Schematic illustrating various functions of the integrated sensors, including sweat UA and Tyr monitoring, sweat rate evaluation, skin temperature perception and vital-sign (for instance, heart rate and respiration rate) detection; (C) Optical photographs of a healthy subject wearing the sensing system at different body positions; (D) Real-time measurement results of multiple physiological signals from a healthy subject during a control exercise process. Reproduced with permission[42]. Copyright 2022, Springer Nature; (E) Schematic of a wearable multimodal sensing system with double-sided modules; (F) Schematic of the functions of the wearable system for human sports monitoring; (G) Indicators (including skin temperature, sweat metabolites, and ECG) of a volunteer recorded by the wearable system under different body status. Reproduced with permission[107]. Copyright 2022, American Chemical Society. LIG: Laser-induced-graphene; UA: uric acid; Tyr: tyrosine; ECG: electrocardiography.

the skin surface of a volunteer to monitor the wrist bending signals. When the device did not capture any signals for a long time, there was feedback to the heater to produce enough heat to wake the person. The heater was switched off when the signal was perceived again, and the temperature would slowly cool down and recover to room temperature [Figure 12D]. The multifunctional device exhibited great potential in intelligent healthcare monitoring and timely management applications.

Benefiting from the thermoacoustic effect, the LIG can function as a micro-speaker, which probably becomes a potential candidate for recovering the communicational abilities of people with phonation-related disabilities. Yang *et al.* reported a LIG-based wearable and smart AT, which could monitor human speech and vocalization-related motions [Figure 12E][46]. The LIG-based AT was conformally integrated with the skin of the larynx, capable of perceiving the tiny mechanical vibrations induced by sound waves and muscle movements. The results revealed that the AT was sensitive to audio up to 2,000 Hz, which

Table 4. Summary of typical LIG-based biochemical sensors for healthcare

LIG composites/substrate	Analytes	Performance	Applications	Ref.
PANI@LIG (E)/PI/Ecoflex	pH	Sensitivity: -53 mV/pH	NA	[41]
PEDOT@LIG (E)/PI	Dopamine	Sensitivity: 0.22 ± 0.01 μA/μM	NA	[75]
Ni@LIG (E), Au@LIG (E)/PI	Glucose	Sensitivity: 1,080 $\mu A \cdot mM^{-1} \cdot cm^{-2}$	Accurate glucose measurements from the human sweat	[40]
FeNCs@LIG (E)/PI	Tyr, UA	Detection limit: Tyr, 5.11 μM; UA 1.37 μM	Accurate detection of Tyr and UA in sweat	[103]
LIG (E)/PI	Cortisol	Assay time: < 1 min	Efficient cortisol sensing in human sweat and saliva	[43]
LIG (E)/PI/Ecoflex	NOx	Sensitivity: NO, 4.18‰ ppm^{-1}; NO_2, 6.66‰ ppm^{-1}	Accurately classify patients with respiratory diseases from healthy human subjects	[39]
LIG (S, E)/PI	Temperature, respiration rate, Tyr, UA	Sensitivity: temperature: -0.06% $°C^{-1}$; UA, 3.50 $\mu A \cdot \mu M^{-1} \cdot cm^{-2}$; Tyr, 0.61 $\mu A \cdot \mu M^{-1} \cdot cm^{-2}$	Gout monitoring in patients and healthy controls	[42]
LIG (S, E)/PI	Strain, pressure, temperature, proximity, ECG, EMG, TENG, Na^+, H^+, Acetone gas, NO_2	Sensitivity: strain, 2.277; pressure, 2.23 MPa^{-1}; temperature, -514.06 ppm $°C^{-1}$; proximity, 1.93% mm^{-1}; pH, -60.91 mV/pH	Depicts the human-ambience interface amid the laboratory and exercising atmosphere	[107]

LIG: Laser-induced-graphene; PANI: polyaniline; PI: polyimides; PEDOT: poly(3,4-ethylenedioxythiophene); FeNCs: iron nano-catalysts; Tyr: tyrosine; UA: uric acid; ECG: electrocardiography; EMG: electromyography; TENG: triboelectric nanogenerator.

covered the frequency range of human voice. Meanwhile, the intelligent AT produced sound through the thermoacoustic effect, converting mechanical information into speech. Driven by a safe voltage of 5 V, the intelligent AT could generate sounds in the 100-20 kHz range and around 60 dB. By incorporating an artificial intelligence model, the intelligent AT device recognized daily words spoken by a patient with a laryngectomy, achieving a high accuracy (> 90%) [Figure 12F]. Furthermore, the recognized words were synthesized into speech and displayed on the AT to rehabilitate the vocalization capability of patients.

Meanwhile, Sun *et al.* developed a LIG-based dual-function acoustic transducer containing a triboelectric artificial ear and a thermoacoustic artificial mouth [Figure 12G][108]. The designed acoustic transducer consisted of three layers: a multi-hole PI sheet with double-side-patterned LIG, a PET ring spacer, and a PI film with one-side-patterned LIG. The input alternating electrical energy was converted into periodic joule heat energy by the thermoacoustic LIG, shrinking air and generating audio waves [Figure 12H]. The fabricated device exhibited ultrahigh sensitivity of 4,500 $mV \cdot Pa^{-1}$, a high resolution of 0.005 Hz, and excellent stability (70-115 dB). Using machine learning, the acoustic transducer could recognize multidimensional speeches with a high accuracy of 96.63% [Figure 12I]. In addition, the device could be utilized for artificial intelligence communication based on detected speech features. Typical LIG-based soft bio-actuators for intelligent healthcare are summarized in Table 5.

LIGS²E for power supply

Power supply devices

Thanks to the fast development of wearable devices and Micro-electromechanical Systems (MEMS) products, there is an urgent demand for soft energy storage devices used for wearable electronics[109-112]. Batteries, fuel cells, and supercapacitors play important roles in electrochemical energy conversion and storage, and TENG provides an effective strategy for mechanical energy conversion[113-119]. The LIG electrodes can enhance their performance from the following aspects: (1) the porous LIG electrodes increase the contact area between electrode and electrolyte, resulting in the improvement of specific capacitance; (2)

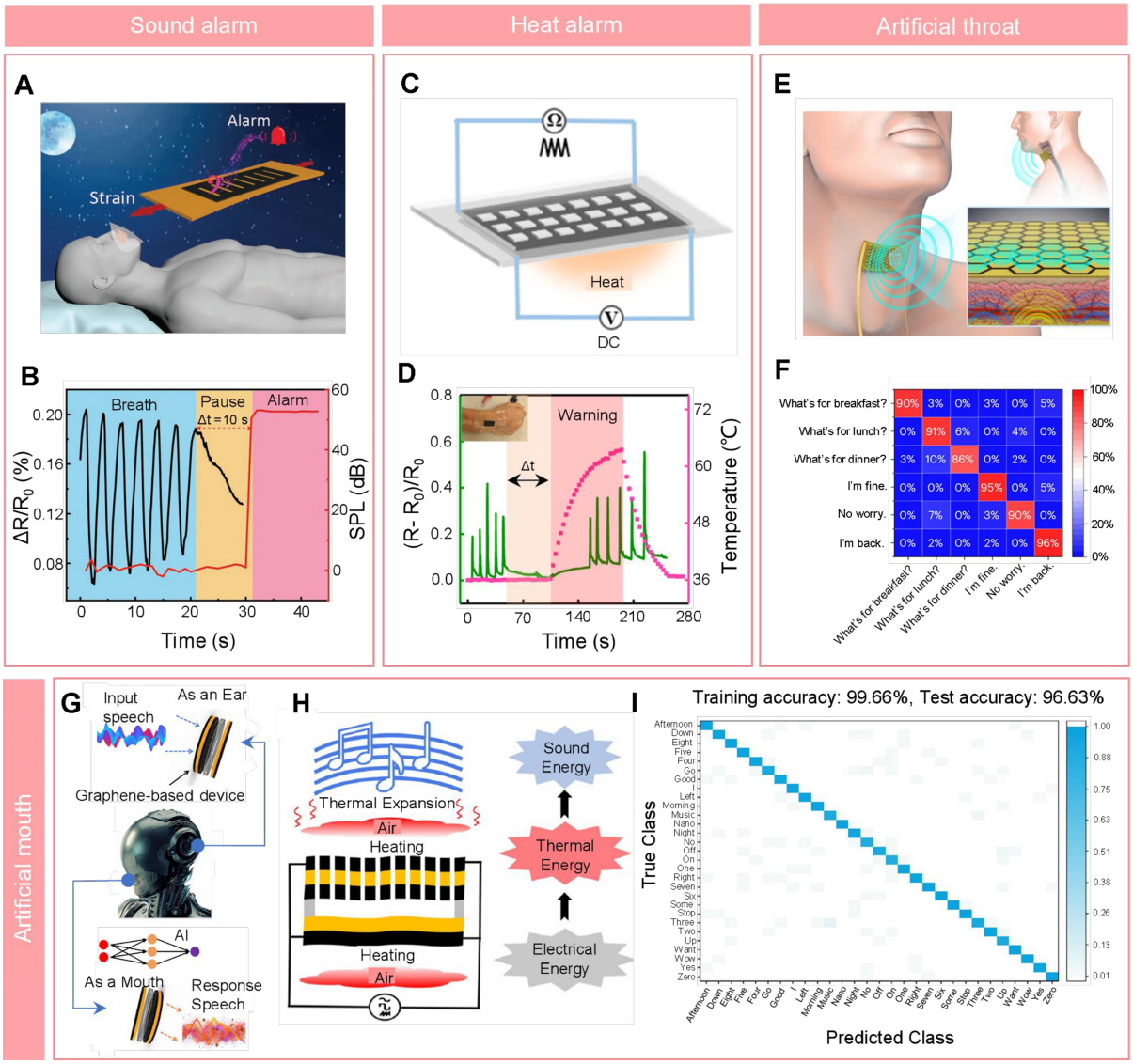

Figure 12. LIG-based skin electronics as bio-actuators for intelligent healthcare. (A) Schematic of a dual functional (monitor and an alarm) E-skin for healthcare; (B) The human experimental results exhibited the E-skin could both detect respiration and sound an alarm; Reproduced with permission[44]. Copyright 2019, Wiley-VCH GmbH; (C) Illustration of a multifunctional device for the sensing and thermal alarm applications; (D) Outputs of the device integrated on the human wrist for the bending detection and thermal alarm modes. Reproduced with permission[45]. Copyright 2020, American Chemical Society; (E) Schematic of an intelligent AT mounted on the skin surface of the larynx; (F) Confusion matrix of several daily sentences produced by an ensemble model. Reproduced with permission[46]. Copyright 2023, Springer Nature; (G) Illustration of LIG-based dual-function acoustic transducers, including an artificial ear and an artificial mouth; (H) The working principles of the device functions as sound emission by thermoacoustic effect; (I) Classification results of speech recognition. Reproduced with permission[108]. Copyright 2023, Wiley-VCH GmbH. LIG: Laser-induced-graphene; E-skin: electric skin; AT: artificial throat.

the micro-structured LIG electrodes strengthen the frictional effect, thereby enhancing the TENG performance.

Lightweight batteries with high energy density can provide a stable power supply for soft-skin electronics. The LIG electrode with porous structures exhibited great potential for developing high-performance batteries. Aslam *et al.* reported a lithium-ion battery based on LIG foams, which functioned as anodes

Table 5. Summary of typical LIG-based soft bio-actuators for intelligent healthcare

Device configuration	Performance	Intelligent healthcare applications	Ref.
Strain sensor/ sound alarm	GF: 316.3; sound generation: 200 Hz - 20 kHz	Health monitoring and alarm of CVD and sleep apnea	[44]
Strain sensor/ heater	GF: 950; temperature range: 25~88.5 °C	Healthcare monitoring and timely warning	[45]
Sound sensor/ artificial throat	Sound detection: 0-2 kHz; sound generation: 100-20 kHz, 60 dB	Recognized daily words vaguely spoken by a patient with laryngectomy	[46]
Pressure sensor/ artificial mouth	Sound sensing sensitivity: 45,000 $mV \cdot Pa^{-1}$; sound-producing frequency range: 20 Hz - 20 kHz	Artificial intelligence communication based on recognized speech features	[108]

LIG: Laser-induced-graphene; GF: gauge factor; CVD: cardiovascular disease.

[Figure 13A][48]. The fabricated lithium-ion battery presented a high reversible areal capacity of approximately 280 $\mu A \cdot h \cdot cm^{-2}$. Furthermore, it exhibited a stable performance for at least 100 cycles with an average coulombic efficiency of 99%. In addition, biochemical energy can be effectively converted into electricity by enzymatic biofuel cells (EBFCs), which probably supplies continuous and stable power outputs for integrated biosensors[120]. Motivated by this, Huang *et al.* developed AuNPs/LIG composites-based transient glucose EBFCs (TEBFCs) [Figure 13B][71]. The AuNPs/LIG electrode exhibited better than the pure LIG electrode, probably due to its low electric impedance and large surface area [Figure 13C]. The developed TEBFC showcased outstanding output performance with an open circuit potential of 0.77 V and a maximum power density of 483.1 $\mu W/cm^2$. Meanwhile, benefiting from poly(lactic-coglycolic acid) (PLGA) substrate, the TEBFCs can be degraded and absorptive inside animal bodies in 44 days. The TEBFC could be a transient power source for low-power implantable bioelectronics.

TENGs can convert external mechanical energy into electricity by combining the triboelectric effect and electrostatic induction[121]. Our daily activities (walking, typing, joint movement, *etc.*) provide a ceaseless mechanical stimulus source for energy collection. Motivated by this, LIG is widely used as electrodes to fabricate high-performance soft skin electronics, collect energy, and record physiological signals. Stanford *et al.* reported a stretchable and flexible single-electrode TENG based on LIG/PDMS composites, generating power by contacting skin[122] [Figure 13D]. The developed LIG/PDMS-based TENG was inserted into a shoe, effectively demonstrating mechanical energy harvesting. The results revealed that the developed TENG showcased a peak power output of 1.2 mW (0.33 Wm^{-2}) as a load resistance of 70 MΩ.

Meanwhile, Das *et al.* created a LIG-based self-powered triboelectric pressure sensor, which consisted of three layers, i.e., a LIG/PI film acting as the bottom electrode, a microstructured PDMS layer, and a PET/ indium tin oxide (ITO) film with opposite triboelectric polarity[49] [Figure 13E]. The fabricated pressure sensor exhibited a fast response time (9.9 ms) and a high sensitivity (7.697 kPa^{-1}), which is beneficial for telemedicine. For instance, a clear pulse waveform could be recorded from a human finger on the pressure sensor. In addition, Yang *et al.* reported a stretchable TENG by integrating AgNWs/LIG electrodes with triboelectric MXene/PDMS-Ecoflex composites for mechanical energy collection and mechanical signal perception[70]. The stretchable AgNWs/LIG electrodes were developed by spray coating the AgNWs on pre-stretched LIG/PDMS-Ecoflex substrates. These electrode designs endowed the developed TENG with stable performance even under 30% tensile strain, outperforming most of the previously related works. Besides, the stretchable TENG can be conformally attached to 3D complicated surfaces, for instance, integrated onto human skin for human movement monitoring [Figure 13F].

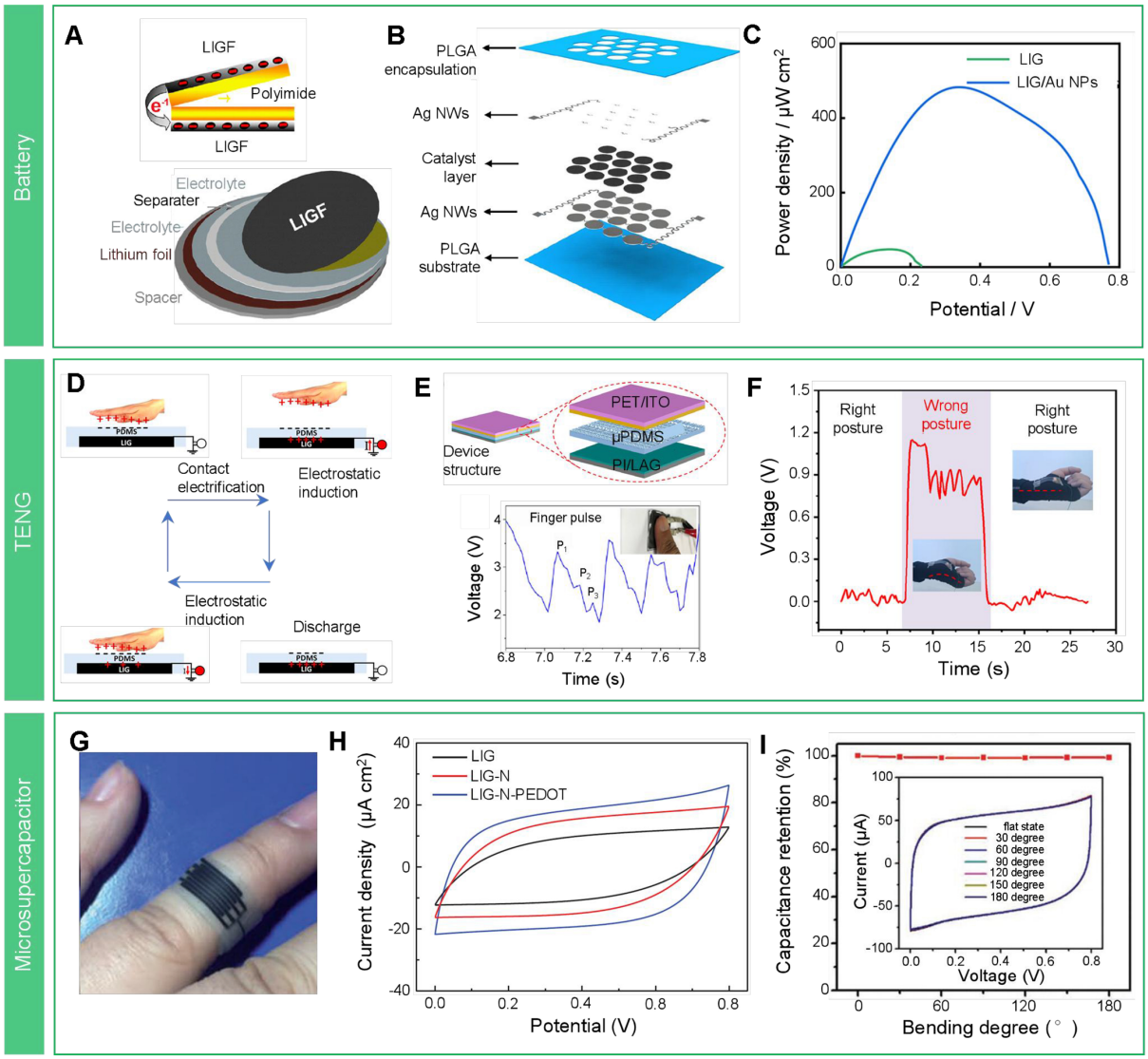

Figure 13. LIG-based soft TENG and supercapacitor are the main constituent parts for the power supply of skin electronics. (A) A LIG-based coin cell. Reproduced with permission[48]. Copyright 2019, Elsevier B.V.; (B and C) A transient and ultrathin biofuel cells enabled by LIG/AuNP composite. Reproduced with permission[71]. Copyright 2022, American Chemical Society; (D) A flexible and stretchable single-electrode TENG based on LIG/PDMS composites. Reproduced with permission[122]. Copyright 2019, American Chemical Society; (E) A flexible triboelectric pressure sensor based on LIG. Reproduced with permission[49]. Copyright 2019, Springer; (F) A stretchable and soft MXene/LIG foam-based TENG for exercise posture detection. Reproduced with permission[70]. Copyright 2022, Elsevier B.V.; (G) A flexible and transparent planar LIG-based microsupercapacitor; (H) C-V plots of microsupercapacitors with different electrode materials. Reproduced with permission[50]. Copyright 2017, Wiley-VCH GmbH; (I) Capacitance retention of LIG-based micro-supercapacitors under different bent states compared to the value in the flat state. Reproduced with permission[31]. Copyright 2019, Wiley-VCH GmbH. LIG: Laser-induced-graphene; TENG: triboelectric nanogenerator; AuNP: gold nanoparticle; PDMS: polydimethylsiloxane.

The converted or collected energy must be stored to provide a stable power supply for wearable electronics. Benefiting from rapid charge-discharge rate, high power density, stability and safety, MSCs have become promising candidates for microscale energy storage devices[123]. The ion adsorption or surface redox reaction at the interface between electrodes and electrolytes implemented the energy storage process. Song *et al.* reported transparent, stretchable, and soft in-plane MSCs based on porous LIG electrodes [Figure 13G][50]. The fabricated device showcased remarkable stretchability up to 400% and long-term stability (1,000 times).

Table 6. Summary of typical LIG-based soft power supply devices

Power supply type	LIG composites/substrate	Working performance	Ref.
Lithium-ion batteries	LIG/PI	Areal capacity: 280 μA·h·cm^{-2}	[48]
Glucose enzymatic biofuel cells	AuNP@LIG/PLGA	maximum power density: 483.1 μW/cm^{2}	[71]
TENG	LIG/PDMS	Power output: 1.2 mW	[122]
TENG	LIG/PDMS	Pressure sensitivity: 7.697 kPa^{-1}	[49]
TENG	AgNWs@LIG/PDMS/Ecoflex	Power: 2.76 W·m^{-2}	[70]
MSC	LIG/Ecoflex	Capacity: 790 μF·cm^{-2}	[50]
MSC	LIG/PI	Areal capacitance: 0.62 mF·cm^{-2}	[31]

LIG: Laser-induced-graphene; PI: polyimides; AuNP: gold nanoparticle; PLGA: poly(lactic-coglycolic acid); TENG: triboelectric nanogenerator; PDMS: polydimethylsiloxane; AgNWs: silver nanowires; MSC: micro-supercapacitor.

The 3D LIG electrode modified by conductive PEDOT could improve the electrical conductivity of electrodes and enhance the capacitance of these planar MSCs [Figure 13H]. The device achieved a specific capacity of 790 μF·cm^{-2} at a discharge current of 50 μA·cm^{-2}. Meanwhile, Shi *et al.* proposed all-solid-state, highly integrated LIG-based MSCs with remarkable pattern variety, outstanding performance uniformity, flexibility, high integration, and exceptional temperature stability[31]. The cyclic voltammetry (CV) tests revealed that the fabricated LIG-based MSCs exhibited high robust stability even when they underwent different bent states from 0° to 180° [Figure 13I]. Furthermore, the developed device showcased remarkable high-temperature performance by combining thermally stabile PI substrates with high-temperature stable ionic liquid electrolytes. Typical LIG-based soft power supply devices for intelligent healthcare are summarized in Table 6.

Standalone LIGS^{2}E

The extensive utilization of soft skin electronics in intelligent healthcare is impeded by challenges on power supply performance and external devices required for data processing and analysis. To tackle this challenge, Zhao *et al.* reported a LIG-based soft and sweat-powered health status sensing and visualization system (HSSVS), which was composed of four sweat-activated batteries (SABs) as power supply modules, three kinds of sensors, a microcontroller unit (MCU), and a specifically designed light-emitting diode (LED) array as a health status visualization component [Figure 14A][124]. The HSSVS system is powered by developed SABs, which achieved a maximum specific capacity of 148.10 mAh·g^{-1} and powered 120 LEDs for over 8 h. In addition, the fabricated system could perceive a series of crucial human physiological indicators, including pH levels, Na^{+} concentration in sweat, and skin temperature. Furthermore, the standalone HSSVS, when attached to the skin surface, validated the excellent potential for continuous visualization of an individual's health status during exercise.

In addition to LIG-based batteries, researchers have developed standalone soft skin electronics by integrating LIG-based TENG as an energy collector and MSCs as energy storage. For instance, Zhang *et al.* reported a porous LIG-based self-powered, wireless, and wearable sensing platform for intelligent health management [Figure 14B][47]. The proposed sensing platform comprised LIG-based TENG for mechanical energy harvesting, microsupercapacitor arrays (MSCAs) based on LIG for energy storage, and multimodal biosensor arrays (including pressure, strain, temperature, ECG, and blood oxygen sensors) for biophysical signals collection. The power supply based on LIG, which combined TENG with MSCAs to harness mechanical energy from human motions for charging, demonstrates the capability to drive integrated biosensors. The developed platform could record pulse waves, strain, temperature, ECG, blood pressure, and blood oxygen from human skin, the monitoring results displayed in a mobile user interface, paving the way for intelligent healthcare.

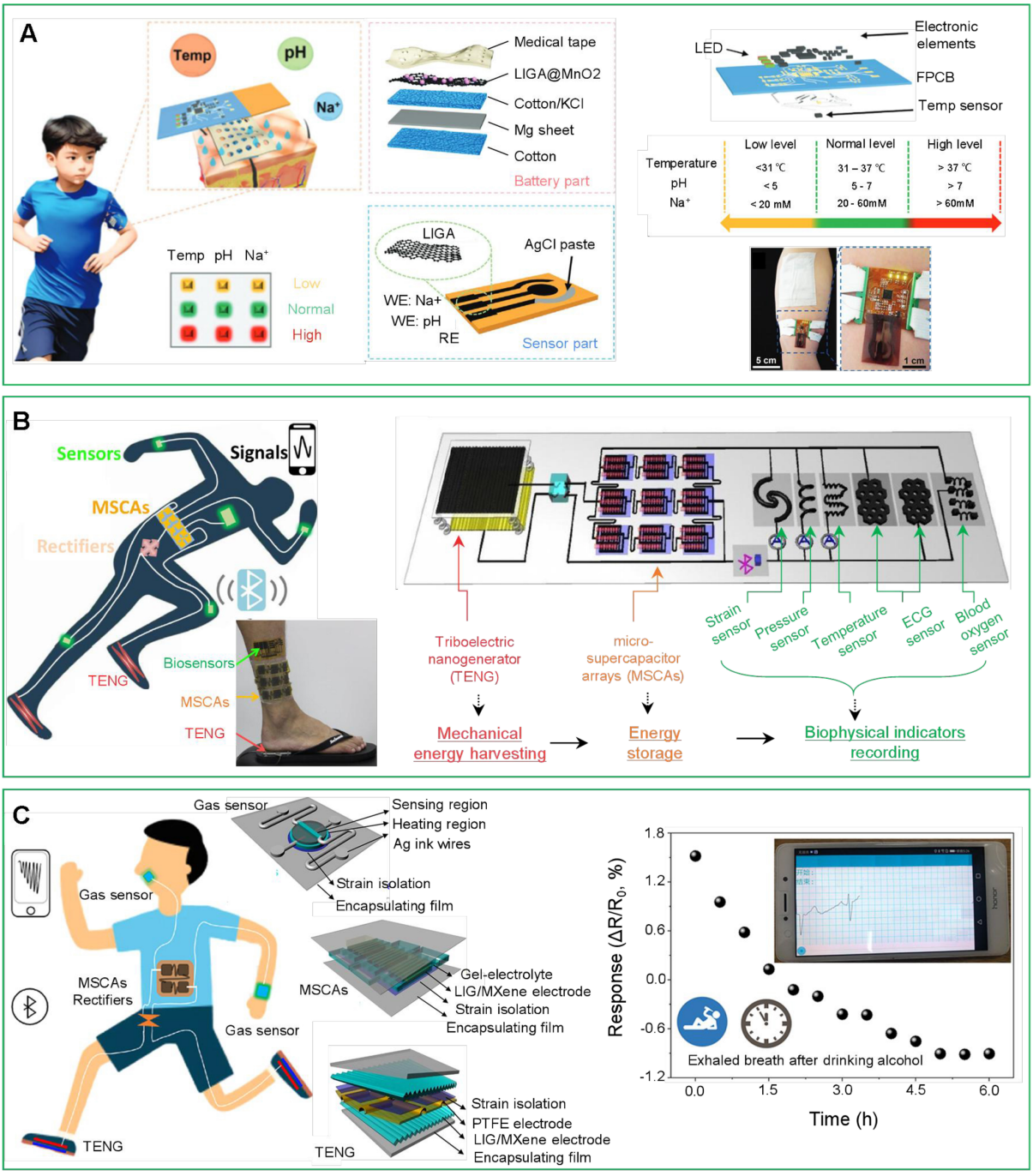

Figure 14. Standalone LIGS^{2}E for intelligent healthcare. (A) A SABs powered HSSVS for health management. Reproduced with permission[124]. Copyright 2023, Wiley-VCH GmbH; (B) LIG-based human motion-driven sensing platform for healthcare. Reproduced with permission[47]. Copyright 2022, AIP Publishing; (C) A fully integrated gas sensing platform based on porous LIG/MXene composites. Reproduced with permission[73]. Copyright 2023, American Chemical Society. LIGS^{2}E: LIG-based soft skin electronics; SABs: sweat-activated batteries; HSSVS: health status sensing and visualization system; LIG: laser-induced-graphene.

Meanwhile, they developed a fully standalone gas sensing system based on crumpled LIG/MXene composites, seamlessly integrating flexible, self-powered units with gas sensors [Figure 14C][73]. The self-powered unit comprises a TENG, power management circuit, and MSCAs. The incorporation of LIG/

MXene composites holds the potential to enhance the performance of the sensing system by capitalizing on the expansive effective triboelectric areas within TENGs, increased electrochemically active sites for electronic charge storage in MSCAs, as well as improved gas molecule adsorption sites and charge transfer processes for gas sensing. Besides, the island-bridge architecture design enabled the system to work under complex mechanical deformations on human skin or clothing. The standalone system achieved wireless, real-time, and continuous monitoring of the exhaled breath flow of the human subject, driven by the integrated self-charging power unit.

Moreover, the island-bridge architecture design of the system enables its functionality even under intricate mechanical deformations when applied to human skin or clothing. The standalone system accomplished wireless and real-time detection of the exhaled breath flow of human subjects, facilitated by the integrated self-charging power units. Typical LIG-based fully standalone systems for intelligent healthcare are summarized in Table 7.

CONCLUSION AND OUTLOOK

Here, we showcase an overview of the recent developments of LIGS²E, including preparation methods, device regulation strategies, and various applications in intelligent healthcare. Although they have achieved rapid and booming advances, the LIGS²E still faces potential challenges in practical applications in intelligent health management.

Firstly, more attention is required on the LIG and device preparation. Though the conductivity of the LIG has improved, it is still far from that of traditional electrodes. Thus, the conductivity and uniformity of LIG should be enhanced, facilitating the development of large-scale soft skin electronics and the integration with commercial MEMS modules. Profited from the facile preparation methods, the soft skin electronics with multiple sensing modes is a promising direction. However, achieving precise decoupling and low crosstalk among sensing elements is still an urgent challenge[93,125].

Then, the degree of intelligence needs to be enhanced, from hardware to software. Integrating multiple sensing modes, wireless modulus, alarm elements, embedded algorithms, and the Internet of Things (IoT) turns the devices into fully standalone systems as intelligent patches. This will establish solid remote monitoring and timely feedback between users and doctors/hospitals. As for the software, artificial intelligence (such as machine learning, deep learning, *etc.*) can facilitate data processing and overall performance enhancement, especially for classification or diagnostics. In addition, suitable algorithm selection can achieve a balance between sample size and calculation accuracy. The introduction of artificial intelligence further facilitates the achievement of intelligent healthcare.

Due to the terminal objectives of soft skin electronics and intelligent healthcare in clinical application, several essential points must be considered. The skin-interfaced devices should be comfortable, lightweight, and have high integration. The device's accuracy must be compared to clinical "standard" equipment/machines. Finally, the performance of the devices should be assessed with extensive clinical cases, improving their practical application capability.

We believe these challenges will be solved well with the endless efforts of scientists from different disciplines, including materials/chemistry, MEMS, mechanics, biology, and computer engineering. The high-performance and cost-effective LIGS²E will give intelligent healthcare a promising prospect, especially for low-income regions.

Table 7. Summary of typical LIG-based fully standalone systems for healthcare

LIG composites (role)/substrate	LIG-based elements	Working performance	Ref.
Au@LIG (S, E), MnO_2@LIG (E)/Ecoflex	TENG, MSC, biosensors (pressure, strain, temperature, ECG, blood oxygen sensor)	Fully standalone system wirelessly measures pulse, strain, temperature, electrocardiogram, blood pressure, and blood oxygen	[124]
LIG/MXene (E)/Ecoflex	TENG, MSC, gas sensor	Monitoring of the exhaled human breath and the local air quality	[47]
LIG (E), MnO_2@LIG (E)/PI	SABs, biosensors (Na^+, pH sensor)	Detection of physiological information: Na^+ concentration and the pH level in sweat, skin temperature	[73]

LIG: Laser-induced-graphene; TENG: triboelectric nanogenerator; MSC: micro-supercapacitor; ECG: electrocardiography; PI: polyimides; SABs: sweat-activated batteries.

DECLARATIONS

Authors' contributions

Initiated the idea, designed and wrote the original draft: Ma Z
Supervised, reviewed and revised the manuscript: Ma Z, Khoo BL

Availability of data and materials

Not applicable.

Financial support and sponsorship

This study was supported by the City University of Hong Kong and funded by the Research Grants Council (RGC). This work was partly supported by the InnoHK Project on Project 1.2 - Novel Drug Delivery Systems to Achieve Precision Medicine for Acute CVD Patients (a closed-loop CVD control system) at the Hong Kong Center for Cerebro-cardiovascular Health Engineering (COCHE). City University of Hong Kong (9610430, 7020002, 9667220), which is funded by the Research Grants Council (RGC); Innovation and Technology Commission (ITC) - Research Talent Hub (RTH) 1-5.

Conflicts of interest

Both authors declared that there are no conflicts of interest.

Ethical approval and consent to participate

We confirmed that the related original figures from referenced studies were approved or exempted by the relevant ethics committee and received the consent to participate from the subjects.

Consent for publication

Not applicable.

REFERENCES

1. Serup J, Jemec GBE, Grove GL. Handbook of non-invasive methods and the skin. 2nd edition. CRC Press: Boca Raton. 2006. DOI
2. Liu Y, Pharr M, Salvatore GA. Lab-on-skin: a review of flexible and stretchable electronics for wearable health monitoring. *ACS Nano* 2017;11:9614-35. DOI PubMed
3. Ma Z, Hua H, You C, et al. FlexiPulse: a machine-learning-enabled flexible pulse sensor for cardiovascular disease diagnostics. *Cell Rep Phys Sci* 2023;4:101690. DOI
4. Guo W, Ma Z, Chen Z, et al. Thin and soft Ti_3C_2Tx MXene sponge structure for highly sensitive pressure sensor assisted by deep learning. *Chem Eng J* 2024;485:149659. DOI
5. Wang Y, Lee S, Yokota T, et al. A durable nanomesh on-skin strain gauge for natural skin motion monitoring with minimum

mechanical constraints. *Sci Adv* 2020;6:eabb7043. DOI PubMed PMC
6. Zhuang M, Yin L, Wang Y, et al. Highly robust and wearable facial expression recognition via deep-learning-assisted, soft epidermal electronics. *Research* 2021;2021:9759601. DOI PubMed PMC
7. Wong TH, Yiu CK, Zhou J, et al. Tattoo-like epidermal electronics as skin sensors for human machine interfaces. *Soft Sci* 2021;1:10. DOI
8. Zhou Z, Chen K, Li X, et al. Sign-to-speech translation using machine-learning-assisted stretchable sensor arrays. *Nat Electron* 2020;3:571-8. DOI
9. Fellmann N, Grizard G, Coudert J. Human frontal sweat rate and lactate concentration during heat exposure and exercise. *J Appl Physiol Respir Environ Exerc Physiol* 1983;54:355-60. DOI PubMed
10. Wang B, Zhao C, Wang Z, et al. Wearable aptamer-field-effect transistor sensing system for noninvasive cortisol monitoring. *Sci Adv* 2022;8:eabk0967. DOI PubMed PMC
11. Lin J, Fu R, Zhong X, et al. Wearable sensors and devices for real-time cardiovascular disease monitoring. *Cell Rep Phys Sci* 2021;2:100541. DOI
12. Chen S, Qi J, Fan S, Qiao Z, Yeo JC, Lim CT. Flexible wearable sensors for cardiovascular health monitoring. *Adv Healthc Mater* 2021;10:e2100116. DOI PubMed
13. Wang C, Sani ES, Gao W. Wearable bioelectronics for chronic wound management. *Adv Funct Mater* 2022;32:2111022. DOI PubMed PMC
14. Ma Y, Zhang Y, Cai S, et al. Flexible hybrid electronics for digital healthcare. *Adv Mater* 2020;32:e1902062. DOI PubMed
15. Gao W, Ota H, Kiriya D, Takei K, Javey A. Flexible electronics toward wearable sensing. *Acc Chem Res* 2019;52:523-33. DOI PubMed
16. Yang JC, Mun J, Kwon SY, Park S, Bao Z, Park S. Electronic skin: recent progress and future prospects for skin-attachable devices for health monitoring, robotics, and prosthetics. *Adv Mater* 2019;31:e1904765. DOI PubMed
17. Yang W, Li N, Zhao S, et al. A breathable and screen-printed pressure sensor based on nanofiber membranes for electronic skins. *Adv Mater Technol* 2018;3:1700241. DOI
18. Sinha AK, Goh GL, Yeong WY, Cai Y. Ultra-low-cost, crosstalk-free, fast-responding, wide-sensing-range tactile fingertip sensor for smart gloves. *Adv Mater Inter* 2022;9:2200621. DOI
19. Cho C, Shin W, Kim M, et al. Monolithically programmed stretchable conductor by laser-induced entanglement of liquid metal and metallic nanowire backbone. *Small* 2022;18:e2202841. DOI PubMed
20. Kim J, Won D, Kim TH, Kim CY, Ko SH. Rapid prototyping and facile customization of conductive hydrogel bioelectronics based on all laser process. *Biosens Bioelectron* 2024;258:116327. DOI PubMed
21. You R, Liu YQ, Hao YL, Han DD, Zhang YL, You Z. Laser fabrication of graphene-based flexible electronics. *Adv Mater* 2020;32:e1901981. DOI PubMed
22. Dong Z, He Q, Shen D, et al. Microfabrication of functional polyimide films and microstructures for flexible MEMS applications. *Microsyst Nanoeng* 2023;9:31. DOI PubMed PMC
23. Lin J, Peng Z, Liu Y, et al. Laser-induced porous graphene films from commercial polymers. *Nat Commun* 2014;5:5714. DOI PubMed PMC
24. Burke M, Larrigy C, Vaughan E, et al. Fabrication and electrochemical properties of three-dimensional (3D) porous graphitic and graphenelike electrodes obtained by low-cost direct laser writing methods. *ACS Omega* 2020;5:1540-8. DOI PubMed PMC
25. Ye R, Chyan Y, Zhang J, et al. Laser-induced graphene formation on wood. *Adv Mater* 2017;29:1702211. DOI PubMed
26. Wang M, Yang Y, Gao W. Laser-engraved graphene for flexible and wearable electronics. *Trend Chem* 2021;3:969-81. DOI
27. Lu Y, Yang G, Wang S, et al. Stretchable graphene–hydrogel interfaces for wearable and implantable bioelectronics. *Nat Electron* 2024;7:51-65. DOI
28. Yu H, Gai M, Liu L, Chen F, Bian J, Huang Y. Laser-induced direct graphene patterning: from formation mechanism to flexible applications. *Soft Sci* 2023;3:4. DOI
29. Zhang S, Zhu J, Zhang Y, et al. Standalone stretchable RF systems based on asymmetric 3D microstrip antennas with on-body wireless communication and energy harvesting. *Nano Energy* 2022;96:107069. DOI
30. Luong DX, Yang K, Yoon J, et al. Laser-induced graphene composites as multifunctional surfaces. *ACS Nano* 2019;13:2579-86. DOI PubMed
31. Shi X, Zhou F, Peng J, Wu R, Wu Z, Bao X. One-step scalable fabrication of graphene-integrated micro-supercapacitors with remarkable flexibility and exceptional performance uniformity. *Adv Funct Mater* 2019;29:1902860. DOI
32. Wang H, Li X, Wang X, Qin Y, Pan Y, Guo X. Somatosensory electro-thermal actuator through the laser-induced graphene technology. *Small* 2024;20:e2310612. DOI PubMed
33. Page MJ, McKenzie JE, Bossuyt PM, et al. The PRISMA 2020 statement: an updated guideline for reporting systematic reviews. *Syst Rev* 2021;10:89. DOI PubMed PMC
34. Dallinger A, Keller K, Fitzek H, Greco F. Stretchable and skin-conformable conductors based on polyurethane/laser-induced graphene. *ACS Appl Mater Interfaces* 2020;12:19855-65. DOI PubMed PMC
35. Gandla S, Naqi M, Lee M, et al. Highly linear and stable flexible temperature sensors based on laser-induced carbonization of polyimide substrates for personal mobile monitoring. *Adv Mater Technol* 2020;5:2000014. DOI
36. Luong DX, Subramanian AK, Silva GAL, et al. Laminated object manufacturing of 3D-printed laser-induced graphene foams. *Adv*

Mater 2018;30:e1707416. DOI PubMed

37. Carvalho AF, Fernandes AJS, Leitão C, et al. Laser-induced graphene strain sensors produced by ultraviolet irradiation of polyimide. *Adv Funct Mater* 2018;28:1805271. DOI
38. Lan L, Le X, Dong H, Xie J, Ying Y, Ping J. One-step and large-scale fabrication of flexible and wearable humidity sensor based on laser-induced graphene for real-time tracking of plant transpiration at bio-interface. *Biosens Bioelectron* 2020;165:112360. DOI PubMed
39. Yang L, Zheng G, Cao Y, et al. Moisture-resistant, stretchable NO_x gas sensors based on laser-induced graphene for environmental monitoring and breath analysis. *Microsyst Nanoeng* 2022;8:78. DOI PubMed PMC
40. Zhu J, Liu S, Hu Z, et al. Laser-induced graphene non-enzymatic glucose sensors for on-body measurements. *Biosens Bioelectron* 2021;193:113606. DOI PubMed PMC
41. Rahimi R, Ochoa M, Tamayol A, Khalili S, Khademhosseini A, Ziaie B. Highly stretchable potentiometric pH sensor fabricated via laser carbonization and machining of carbon-polyaniline composite. *ACS Appl Mater Interfaces* 2017;9:9015-23. DOI PubMed
42. Yang Y, Song Y, Bo X, et al. A laser-engraved wearable sensor for sensitive detection of uric acid and tyrosine in sweat. *Nat Biotechnol* 2020;38:217-24. DOI PubMed
43. Torrente-Rodríguez RM, Tu J, Yang Y, et al. Investigation of cortisol dynamics in human sweat using a graphene-based wireless mHealth system. *Matter* 2020;2:921-37. DOI PubMed PMC
44. Chen X, Luo F, Yuan M, et al. A dual-functional graphene-based self-alarm health-monitoring e-skin. *Adv Funct Mater* 2019;29:1904706. DOI
45. Huang Y, Tao LQ, Yu J, Wang Z, Zhu C, Chen X. Integrated sensing and warning multifunctional devices based on the combined mechanical and thermal effect of porous graphene. *ACS Appl Mater Interfaces* 2020;12:53049-57. DOI PubMed
46. Yang Q, Jin W, Zhang Q, et al. Mixed-modality speech recognition and interaction using a wearable artificial throat. *Nat Mach Intell* 2023;5:169-80. DOI
47. Zhang C, Chen H, Ding X, et al. Human motion-driven self-powered stretchable sensing platform based on laser-induced graphene foams. *Appl Phys Rev* 2022;9:011413. DOI
48. Aslam S, Sagar RUR, Liu Y, et al. Graphene decorated polymeric flexible materials for lightweight high areal energy lithium-ion batteries. *Appl Mater Today* 2019;17:123-9. DOI
49. Das PS, Chhetry A, Maharjan P, Rasel MS, Park JY. A laser ablated graphene-based flexible self-powered pressure sensor for human gestures and finger pulse monitoring. *Nano Res* 2019;12:1789-95. DOI
50. Song W, Zhu J, Gan B, et al. Flexible, stretchable, and transparent planar microsupercapacitors based on 3D porous laser-induced graphene. *Small* 2018;14:1702249. DOI PubMed
51. Le TSD, Phan HP, Kwon S, et al. Recent advances in laser-induced graphene: mechanism, fabrication, properties, and applications in flexible electronics. *Adv Funct Mater* 2022;32:2205158. DOI
52. Sharma CP, Arnusch CJ. Laser-induced graphene composite adhesive tape with electro-photo-thermal heating and antimicrobial capabilities. *Carbon* 2022;196:102-9. DOI
53. Yang W, Zhao W, Li Q, et al. Fabrication of smart components by 3D printing and laser-scribing technologies. *ACS Appl Mater Interfaces* 2020;12:3928-35. DOI PubMed
54. Le TD, Park S, An J, Lee PS, Kim Y. Ultrafast laser pulses enable one-step graphene patterning on woods and leaves for green electronics. *Adv Funct Mater* 2019;29:1902771. DOI
55. Jung Y, Min J, Choi J, et al. Smart paper electronics by laser-induced graphene for biodegradable real-time food spoilage monitoring. *Appl Mater Today* 2022;29:101589. DOI
56. Chyan Y, Ye R, Li Y, Singh SP, Arnusch CJ, Tour JM. Laser-induced graphene by multiple lasing: toward electronics on cloth, paper, and food. *ACS Nano* 2018;12:2176-83. DOI PubMed
57. Kim D, Lee H, Hwang E, Hong S, Lee H. Pyrolytic jetting of highly porous laser-induced graphene fiber for cost-effective supercapacitor. *Int J Precis Eng Man* 2024;11:439-47. DOI
58. Chen X, Li R, Niu G, et al. Porous graphene foam composite-based dual-mode sensors for underwater temperature and subtle motion detection. *Chem Eng J* 2022;444:136631. DOI
59. Yang J, Zhang K, Yu J, et al. Facile fabrication of robust and reusable PDMS supported graphene dry electrodes for wearable electrocardiogram monitoring. *Adv Mater Technol* 2021;6:2100262. DOI
60. Kaidarova A, Alsharif N, Oliveira BNM, et al. Laser-printed, flexible graphene pressure sensors. *Glob Chall* 2020;4:2000001. DOI PubMed PMC
61. d'Amora M, Lamberti A, Fontana M, Giordani S. Toxicity assessment of laser-induced graphene by zebrafish during development. *J Phys Mater* 2020;3:034008. DOI
62. Huang L, Xu S, Wang Z, et al. Self-reporting and photothermally enhanced rapid bacterial killing on a laser-induced graphene mask. *ACS Nano* 2020;14:12045-53. DOI PubMed
63. Huang L, Gu M, Wang Z, et al. Highly efficient and rapid inactivation of coronavirus on non-metal hydrophobic laser-induced graphene in mild conditions. *Adv Funct Mater* 2021;31:2101195. DOI PubMed PMC
64. Le TD, Lee YA, Nam HK, et al. Green flexible graphene–inorganic-hybrid micro-supercapacitors made of fallen leaves enabled by ultrafast laser pulses. *Adv Funct Mater* 2022;32:2107768. DOI
65. Yi J, Chen J, Yang Z, et al. Facile patterning of laser-induced graphene with tailored Li nucleation kinetics for stable lithium-metal

batteries. *Adv Energy Mater* 2019;9:1901796. DOI

66. Stanford MG, Zhang C, Fowlkes JD, et al. High-resolution laser-induced graphene. Flexible electronics beyond the visible limit. *ACS Appl Mater Interfaces* 2020;12:10902-7. DOI PubMed
67. Duy LX, Peng Z, Li Y, Zhang J, Ji Y, Tour JM. Laser-induced graphene fibers. *Carbon* 2018;126:472-9. DOI
68. Rahimi R, Ochoa M, Yu W, Ziaie B. Highly stretchable and sensitive unidirectional strain sensor via laser carbonization. *ACS Appl Mater Interfaces* 2015;7:4463-70. DOI PubMed
69. Zang X, Shen C, Chu Y, et al. Laser-induced molybdenum carbide-graphene composites for 3D foldable paper electronics. *Adv Mater* 2018;30:e1800062. DOI PubMed
70. Yang L, Liu C, Yuan W, et al. Fully stretchable, porous MXene-graphene foam nanocomposites for energy harvesting and self-powered sensing. *Nano Energy* 2022;103:107807. DOI
71. Huang X, Li H, Li J, et al. Transient, implantable, ultrathin biofuel cells enabled by laser-induced graphene and gold nanoparticles composite. *Nano Lett* 2022;22:3447-56. DOI PubMed
72. Sharma S, Pradhan GB, Jeong S, Zhang S, Song H, Park JY. Stretchable and all-directional strain-insensitive electronic glove for robotic skins and human-machine interfacing. *ACS Nano* 2023;17:8355-66. DOI PubMed
73. Zhang C, Chen J, Gao J, et al. Laser processing of crumpled porous graphene/MXene nanocomposites for a standalone gas sensing system. *Nano Lett* 2023;23:3435-43. DOI PubMed
74. Zhang S, Chhetry A, Zahed MA, et al. On-skin ultrathin and stretchable multifunctional sensor for smart healthcare wearables. *npj Flex Electron* 2022;6:11. DOI
75. Xu G, Jarjes ZA, Desprez V, Kilmartin PA, Travas-Sejdic J. Sensitive, selective, disposable electrochemical dopamine sensor based on PEDOT-modified laser scribed graphene. *Biosens Bioelectron* 2018;107:184-91. DOI PubMed
76. Heikenfeld J, Jajack A, Rogers J, et al. Wearable sensors: modalities, challenges, and prospects. *Lab Chip* 2018;18:217-48. DOI PubMed PMC
77. Kaidarova A, Khan MA, Marengo M, et al. Wearable multifunctional printed graphene sensors. *npj Flex Electron* 2019;3:15. DOI
78. Xu K, Lu Y, Honda S, Arie T, Akita S, Takei K. Highly stable kirigami-structured stretchable strain sensors for perdurable wearable electronics. *J Mater Chem C* 2019;7:9609-17. DOI
79. Ling Y, Zhuang X, Xu Z, et al. Mechanically assembled, three-dimensional hierarchical structures of cellular graphene with programmed geometries and outstanding electromechanical properties. *ACS Nano* 2018;12:12456-63. DOI PubMed
80. Zhu Y, Cai H, Ding H, Pan N, Wang X. Fabrication of low-cost and highly sensitive graphene-based pressure sensors by direct laser scribing polydimethylsiloxane. *ACS Appl Mater Interfaces* 2019;11:6195-200. DOI PubMed
81. Wang H, Zhao Z, Liu P, Guo X. A soft and stretchable electronics using laser-induced graphene on polyimide/PDMS composite substrate. *npj Flex Electron* 2022;6:26. DOI
82. Jeong SY, Lee JU, Hong SM, et al. Highly skin-conformal laser-induced graphene-based human motion monitoring sensor. *Nanomaterials* 2021;11:951. DOI PubMed PMC
83. Sun B, McCay RN, Goswami S, et al. Gas-permeable, multifunctional on-skin electronics based on laser-induced porous graphene and sugar-templated elastomer sponges. *Adv Mater* 2018;30:e1804327. DOI PubMed
84. Sindhu B, Kothuru A, Sahatiya P, Goel S, Nandi S. Laser-induced graphene printed wearable flexible antenna-based strain sensor for wireless human motion monitoring. *IEEE Trans Electron Devices* 2021;68:3189-94. DOI
85. Luo S, Hoang PT, Liu T. Direct laser writing for creating porous graphitic structures and their use for flexible and highly sensitive sensor and sensor arrays. *Carbon* 2016;96:522-31. DOI
86. Mehmood A, Mubarak NM, Khalid M, Jagadish P, Walvekar R, Abdullah EC. Graphene/PVA buckypaper for strain sensing application. *Sci Rep* 2020;10:20106. DOI PubMed PMC
87. Jeong SY, Ma YW, Lee JU, Je GJ, Shin BS. Flexible and highly sensitive strain sensor based on laser-induced graphene pattern fabricated by 355 nm pulsed laser. *Sensors* 2019;19:4867. DOI PubMed PMC
88. Wei S, Liu Y, Yang L, et al. Flexible large e-skin array based on patterned laser-induced graphene for tactile perception. *Sensor Actuat A Phys* 2022;334:113308. DOI
89. Yoon H, Lee K, Shin H, et al. In situ co-transformation of reduced graphene oxide embedded in laser-induced graphene and full-range on-body strain sensor. *Adv Funct Mater* 2023;33:2300322. DOI
90. Shao Q, Liu G, Teweldebrhan D, Balandin AA. High-temperature quenching of electrical resistance in graphene interconnects. *Appl Phys Lett* 2008;92:202108. DOI
91. Kulyk B, Silva BFR, Carvalho AF, et al. Laser-induced graphene from paper by ultraviolet irradiation: humidity and temperature sensors. *Adv Mater Technol* 2022;7:2101311. DOI
92. Tian Q, Yan W, Li Y, Ho D. Bean pod-inspired ultrasensitive and self-healing pressure sensor based on laser-induced graphene and polystyrene microsphere sandwiched structure. *ACS Appl Mater Interfaces* 2020;12:9710-7. DOI PubMed
93. Li Y, Long J, Chen Y, Huang Y, Zhao N. Crosstalk-free, high-resolution pressure sensor arrays enabled by high-throughput laser manufacturing. *Adv Mater* 2022;34:e2200517. DOI PubMed
94. Marengo M, Marinaro G, Kosel J. Flexible temperature and flow sensor from laser-induced graphene. In: 2017 IEEE SENSORS; 2017 Oct 29 - Nov 01; Glasgow, UK. IEEE; 2017. p. 1-3. DOI
95. Wang J, Wang N, Xu D, Tang L, Sheng B. Flexible humidity sensors composed with electrodes of laser induced graphene and sputtered sensitive films derived from poly(ether-ether-ketone). *Sensor Actuat B Chem* 2023;375:132846. DOI

96. Liu S, Chen R, Chen R, et al. Facile and cost-effective fabrication of highly sensitive, fast-response flexible humidity sensors enabled by laser-induced graphene. *ACS Appl Mater Interfaces* 2023;15:57327-37. DOI PubMed
97. Xu K, Fujita Y, Lu Y, et al. A wearable body condition sensor system with wireless feedback alarm functions. *Adv Mater* 2021;33:e2008701. DOI
98. Babatain W, Buttner U, El-Atab N, Hussain MM. Graphene and liquid metal integrated multifunctional wearable platform for monitoring motion and human-machine interfacing. *ACS Nano* 2022;16:20305-17. DOI PubMed
99. Moin A, Zhou A, Rahimi A, et al. A wearable biosensing system with in-sensor adaptive machine learning for hand gesture recognition. *Nat Electron* 2021;4:54-63. DOI
100. Yang H, Li J, Lim KZ, et al. Automatic strain sensor design via active learning and data augmentation for soft machines. *Nat Mach Intell* 2022;4:84-94. DOI
101. Lu Y, Kong D, Yang G, et al. Machine learning-enabled tactile sensor design for dynamic touch decoding. *Adv Sci* 2023;10:e2303949. DOI PubMed PMC
102. Xie J, Zhao Y, Zhu D, et al. A machine learning-combined flexible sensor for tactile detection and voice recognition. *ACS Appl Mater Interfaces* 2023;15:12551-9. DOI PubMed
103. Zhao P, Zhang Y, Liu Y, Huo D, Hou J, Hou C. Wearable electrochemical patch based on iron nano-catalysts incorporated laser-induced graphene for sweat metabolites detection. *Biosens Bioelectron* 2024;249:116012. DOI PubMed
104. Ricciardolo FL, Sorbello V, Ciprandi G. FeNO as biomarker for asthma phenotyping and management. *Allergy Asthma Proc* 2015;36:e1-8. DOI PubMed
105. Antus B, Barta I, Horvath I, Csiszer E. Relationship between exhaled nitric oxide and treatment response in COPD patients with exacerbations. *Respirology* 2010;15:472-7. DOI PubMed
106. Malerba M, Radaeli A, Olivini A, et al. Exhaled nitric oxide as a biomarker in COPD and related comorbidities. *Biomed Res Int* 2014;2014:271918. DOI PubMed PMC
107. Wang H, Xiang Z, Zhao P, et al. Double-sided wearable multifunctional sensing system with anti-interference design for human-ambience interface. *ACS Nano* 2022;16:14679-92. DOI PubMed
108. Sun H, Gao X, Guo L, et al. Graphene-based dual-function acoustic transducers for machine learning-assisted human–robot interfaces. *InfoMat* 2023;5:e12385. DOI
109. Song W, Wang H, Liu G, Peng M, Zou D. Improving the photovoltaic performance and flexibility of fiber-shaped dye-sensitized solar cells with atomic layer deposition. *Nano Energy* 2016;19:1-7. DOI
110. Pu X, Song W, Liu M, et al. Wearable power-textiles by integrating fabric triboelectric nanogenerators and fiber-shaped dye-sensitized solar cells. *Adv Energy Mater* 2016;6:1601048. DOI
111. Jung S, Lee J, Hyeon T, Lee M, Kim DH. Fabric-based integrated energy devices for wearable activity monitors. *Adv Mater* 2014;26:6329-34. DOI PubMed
112. Lee JW, Xu R, Lee S, et al. Soft, thin skin-mounted power management systems and their use in wireless thermography. *Proc Natl Acad Sci U S A* 2016;113:6131-6. DOI PubMed PMC
113. Liu C, Neale ZG, Cao G. Understanding electrochemical potentials of cathode materials in rechargeable batteries. *Mater Today* 2016;19:109-23. DOI
114. Cong HP, Chen JF, Yu SH. Graphene-based macroscopic assemblies and architectures: an emerging material system. *Chem Soc Rev* 2014;43:7295-325. DOI PubMed
115. Aricò AS, Bruce P, Scrosati B, Tarascon JM, van Schalkwijk W. Nanostructured materials for advanced energy conversion and storage devices. *Nat Mater* 2005;4:366-77. DOI PubMed
116. Pu X, Liu M, Li L, et al. Wearable textile-based in-plane microsupercapacitors. *Adv Energy Mater* 2016;6:1601254. DOI
117. Wang J, Li X, Zi Y, et al. A flexible fiber-based supercapacitor-triboelectric-nanogenerator power system for wearable electronics. *Adv Mater* 2015;27:4830-6. DOI PubMed
118. Wang H, Yang Y, Guo L. Nature-inspired electrochemical energy-storage materials and devices. *Adv Energy Mater* 2017;7:1601709. DOI
119. Zhou L, Zhuang Z, Zhao H, Lin M, Zhao D, Mai L. Intricate hollow structures: controlled synthesis and applications in energy storage and conversion. *Adv Mater* 2017;29:1602914. DOI PubMed
120. Yu Y, Nassar J, Xu C, et al. Biofuel-powered soft electronic skin with multiplexed and wireless sensing for human-machine interfaces. *Sci Robot* 2020;5:eaaz7946. DOI PubMed PMC
121. Chen J, Wang ZL. Reviving vibration energy harvesting and self-powered sensing by a triboelectric nanogenerator. *Joule* 2017;1:480-521. DOI
122. Stanford MG, Li JT, Chyan Y, Wang Z, Wang W, Tour JM. Laser-induced graphene triboelectric nanogenerators. *ACS Nano* 2019;13:7166-74. DOI PubMed
123. Wang G, Zhang L, Zhang J. A review of electrode materials for electrochemical supercapacitors. *Chem Soc Rev* 2012;41:797-828. DOI PubMed
124. Zhao G, Park W, Huang X, et al. Soft, sweat-powered health status sensing and visualization system enabled by laser-fabrication. *Adv Sensor Res* 2023;2:2300070. DOI
125. Yang R, Zhang W, Tiwari N, Yan H, Li T, Cheng H. Multimodal sensors with decoupled sensing mechanisms. *Adv Sci* 2022;9:e2202470. DOI PubMed PMC